An Experimental Evaluation of Passive Cooling Configuration for Improving Solar PV systems Efficiency

Submitted By

Kazi Fahad Labib Timur (180011201)

Tahiya Hossain (180011233)

Mostofa Jahid Saif (180011133)

Supervised By

Prof. Dr. Md. Hamidur Rahman

A Thesis submitted in partial fulfillment of the requirement for the degree of Bachelor of Science in Mechanical Engineering

Department of Mechanical and Production Engineering (MPE)

Islamic University of Technology (IUT)

5th June 2023

Candidate's Declaration

This is to certify that the work presented in this thesis, titled, "An Experimental Evaluation of Passive Cooling Configuration for Improving solar PV systems Efficiency", is the outcome of the investigation and research carried out by me under the supervision of Prof. Dr. Md. Hamidur Rahman.

It is also declared that neither this thesis nor any part of it has been submitted elsewhere for the award of any degree or diploma.

Kazi Fahad Labib Timur

Student No: 180011201

Tahiya Hossain

Student No: 180011233
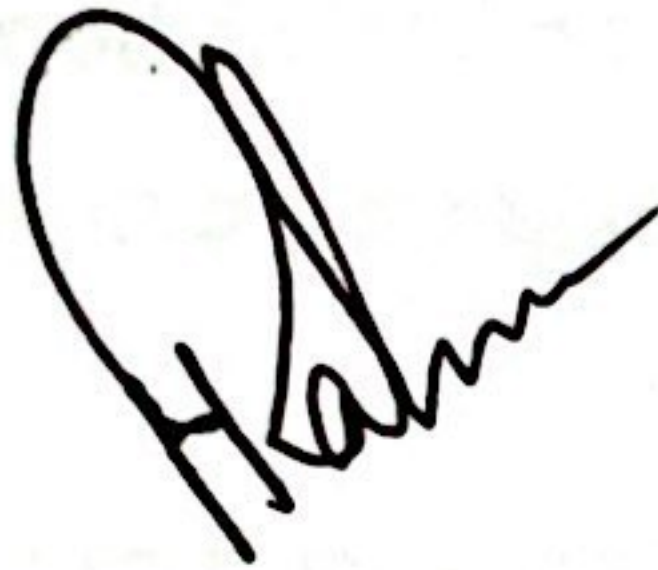

Mostofa Jahid Saif

Student No: 180011133

RECOMMENDATION OF THE BOARD OF SUPERVISORS

The thesis titled "An Experimental Evaluation of Passive Cooling Configuration for Improving Solar PV systems Efficiency" submitted by *Kazi Fahad Labib Timur, Student No: 180011201, Tahiya Hossain, Student No: 180011233, Mostofa Jahid Saif, Student No: 180011133* has been accepted as satisfactory in partial fulfillment of the requirements for the degree of B Sc. in Mechanical Engineering on 12th January 2023.

BOARD OF EXAMINERS

Prof. Dr. Md. Hamidur Rahman   (Supervisor)

Professor

MPE Dept., IUT, Board Bazar, Gazipur-1704, Bangladesh.

3

Acknowledgment

In the Name of Allah, the Most Merciful, the Most Beneficent. First and foremost, I am grateful to ALLAH (SWT), the most merciful and kind, for providing me with the strength and ability to write this thesis. I would like to thank my project supervisor, Prof. Dr. Md. Hamidur Rahman Sir, for his steadfast and patient support throughout the project's unforeseeable complications and for his invaluable suggestions when I encountered obstacles. His generosity, friendliness, and solid supervision at work helped me feel less worried while dealing with unanticipated difficulties and more productive in my personal life.

In the following section, I would want to express my gratitude to my parents for their continuing support and commitment to my higher education.

Abstract

As fossil fuel reserves decline and their environmental impact becomes more apparent, the world is increasingly turning to solar energy as a replacement. To convert photons into electricity, fuel, and heat, however, is necessary for solar energy to become a viable source of energy. The efficiency of photovoltaic (PV) cells used to harvest solar energy ranges between 12 and 25 percent and decreases as their surface temperature increases. Maintaining the PV module's temperature as low as possible is essential to guarantee its durability and performance.

To address this issue, we conducted an experimental analysis to develop a photovoltaic (PV) module with an incorporated passive cooling mechanism. A literature review on solar panel passive cooling disclosed a variety of heat sink configurations. However, the objective of our research is to optimize the design of heat sinks to increase their efficacy while decreasing their material and weight requirements. Our efforts are focused on producing a simple heat sink that is easy to install and put into action while simultaneously improving the overall performance of the PV system.

When the weight of the heat sink is decreased, the amount of material required drops, which results in a solution that is both more environmentally friendly and more cost-effective. Our approach to the construction of a heat absorber that is optimized has the potential to make solar energy more accessible and more economically viable for a larger number of end users.

Contents

1. Nomenclature and Symbol

Symbols	Description
q	Rate of Heat transfer
h_c	Convective heat-transfer coefficient
q_{COND}	Conduction heat-transfer rate
q_{CONV}	Convection heat-transfer rate
q_{RAD}	Radiation heat-transfer rate
P_{MPP}	Maximum power point
T_a	Ambient temperature
T_C	Cold temperature
T_H	High temperature
PV/T	Photovoltaic thermal collector
ε	Emissivity
η	Electric efficiency

Section 1.1 Subscripts

c = convection

COND = conduction

CONV = convection

E = ethyl vinyl acetate (EVA)

G = glass cover

H = heat sink

P = PVF

RAD = radiation

This flowchart depicts the overarching structure of the Study Procedure for this experimental analysis.

Literature Review	■ **Identifying Problems** ■ **Reviewing recently publishhed works** ■ **For experimental investigation, reviewing heat sink passive cooling solutions**
Geometry Selection	**Selection of two heat sink configurations-** ■ **Fin with holes** ■ **Fin with out holes**
Developing Experimental Setup	**Development of the comparative study setup . Experimental setup to collecct real data**
Data collection	**7 to 10 days collection of data for both the heat sinks.**
Comparative study and Result	**Comparison of the acquired data and to determine whether the heat sink is improving the efficiency of the solar panel**

2. Introduction

Section 2.1 Objectives of the Study

Establishing specific objectives or targets is a method for conducting experimental research. Researchers can substantially improve the quality of their work by establishing specific objectives. In this context, the objective of the research is to investigate the effectiveness of a heat sink configuration in enhancing the thermal efficiency of photovoltaic (PV) cells.

Experimenting with heat sink configurations, comparing the voltage and current output of PV cells integrated with and without a heat sink, comparing the thermal efficiency of PV cells integrated with and without a heat sink, and reducing the rate at which the solar PV cell's efficiency decreases as the temperature rises are among the research objectives.

The primary objectives of this experiment were to construct a solar PV panel with an integrated heat sink capable of producing a constant output with the same amount of irradiance and to validate the heat sink model through numerical analysis experimentally. The ultimate objective is to develop a solar module that does not lose efficiency as temperature increases. These objectives have a substantial impact on the experimental analysis and study implementation.

Section 2.2 Background of the study

Renewable energy is the only viable solution to the growing requirement for energy. As non-renewable energy is limited, day by day, the world is getting more dependent on natural sources of energy. Currently, non-renewable energy such as fossil fuels supplies around 80% of the world's energy [1]. In addition to providing us with the energy that we need to survive, non-renewable energy also contributes to environmental harm that has a negative impact on humanity. Due to the combustion of fossil fuels, carbon dioxide gets released into the air, which is the main cause of global warming [2]. The global average temperature has risen 1°C therefore, which is just one of the examples among several other detrimental effects of non-renewable energy [3].

One of the largest major renewables is Solar energy, and its abundance makes its application more practicable. Radiation from the sun is the basis of solar irradiation, which is used to create heat, power generation, and chemical reactions. The amount of energy that Earth receives from the sun outpaces the planet's current and future requirements for energy [4]. Photovoltaic (PV) and solar thermal power systems are the two primary categories of solar power based electricity generation methods [5]. Working on technologies that can be applied to renewable energies is therefore seen

as cutting-edge technology. Energy gained from the sun that continuously impacts the Earth is 1.73 x 105 terawatts (TW), while the average worldwide demand for power is 2.7 TW [6]. However, the conventional PV technology that has been used thus far prevents us from utilizing this energy. The goal of this experiment is increasing the PV system conversion efficiency, which is defined as the proportion of incident irradiation converted to electricity.

PV temperature has a major effect on PV cell efficiency. Solar cell performance decreases with increasing temperature and will produce less energy. As the overall power generation is negatively affected, it is needed to work on the technology that will help the temperature reduction of module. One of the constructive ways to reduce the PV cells temperature is the passive cooling of solar panels. The importance of passive cooling is that no external device is needed, for active cooling forced convection is needed. The efficacy of such elements used in passive cooling is highly dependent on their design and working situations, necessitating the execution of specialized research to demonstrate their viability. And in forced convection, external devices are needed for cooling that will also need energy to run, which will be the opposite of our energy production idea. Heatsinks are used for passive cooling, and if the efficiencies of the PV cells are increased, they can extract more energy from solar radiation [7].

Section 2.3 Literature Review

PV cell performance and efficiency

Although photovoltaic (PV) systems are increasingly employed to generate electricity, the conversion efficiency with most industrial photovoltaic panels is still quite poor, at about 13% to 20% under optimum operating conditions [8]. Due to the correlation between photovoltaic cells' performance and PV cell working temperature, ambient temperature plays a significant role in the overall efficiency of PV systems. The remaining irradiation is dissipated as heat that enhances cell temperature and, as a result, affects cell output voltage and output power [9].

The PV systems performance declines when they are exposed to environmental factors. Several types of deterioration, including structural failure, critical heat flux, problems with corrosion, broken glass, electricity flowing between units, fading, have been linked to elevated temperatures [10]. Crystalline silicon PV cell modules have become the industry standard for both economic and practical reasons. The electrical efficiency of crystalline silicon cells may decrease by 0.5% for every 1K temperature increase [11]. There are two components to a PV cell's effectiveness:

electrical efficiency and thermal efficiency. In contrast to solar irradiation, the observations of these two types of efficiency are inverse.

The heat transport and energy translation of PV cells are subject to several parameters, which can lead to significant variations in actual-world solar panel performance. Typical polycrystalline PV cells convert only about 15% of incident light into useable energy, while organic PV cells can reach up to 17% [12]. Solar energy conversion to heat can have a significant negative effect on PV cell efficiency, in addition to material constraints in the power transmission capabilities of the PV cells. Additionally, the increased temperatures impact the properties of materials of PV modules. It is challenging to achieve consistent temperature distribution across the surface the modules surface area since the material condition declines over the duration.

Various cooling technologies for rising temperature of PV system

Decreasing the surface temperature of a Photovoltaic panel is an efficient strategy for reducing the speed of thermal damage. To accomplish this, the system must be cooled and kept from overheating while in use [13]. In addition to passive cooling with heat sinks, a PV system may employ several other cooling methods.

The PVT is a piece of equipment that combines a photovoltaic (PV) module converts solar energy into electricity, and a panel with higher heat efficiency, that utilizes a thermal liquid. Rekha et al. [14] simulated and tested a forced convection PV/T system using CFD software. The verified model examined how mass air flow and channel depth affects PV/T performance. The proposed design outperformed a PV/T air collector by 20%.

Phase change materials, which have excellent energy storage and can operate at a constant temperature, have been widely used for the thermal management of PV solar cells. Many studies tested PCM with PV systems. Paraffin is a good phase change material (PCM) because it freezes without supercooling and is available in a wide temperature range [15].

Another cooling method is the jet impingement system. An impingement cooling system shoots high-velocity fluid jets at a target. Submerged or free jets can impinge. Bahaidarah et al. [16] examined how temperature dispersion affects cooled PV systems. Jet cooling outperformed heat

exchangers in efficiency, lowest cell temperature, and homogeneity. Jet cooling with homogeneous heat transfer cools each cell independently.

To increase the sun's energy output from 200 suns to 1000 W/m^2, concentrating photovoltaic systems (CPV) use relatively cheap Fresnel lenses or mini reflectors. Heat pipes could passively extract excess heat off CPV cells with high heat flux and discard it into the environment through natural convection. Anderson et al. [17] proposed cooling CPV cells by natural convection with a copper water heat pipe where he used aluminum fins. The heat pipe heat sinks discarded 40°C of heat into the surroundings utilizing means of natural convection.

Water immersion cooling can regulate surface temperature and improve efficiency at severe temperatures. Saurabh et al. [18] found that cooling improves solar cell electrical efficiency. Under real-world conditions, a solar cell immersed in water can be adjusted from 31 to 39 °C. Cell performance improves greatly. Panel efficiency rose 17.8% at 1cm water depth. Submerging solar cells in diverse fluids supports the Concentrated Photovoltaics System.

Microchannel cooling for photovoltaic panels has a high thermal capacity and has been the subject of substantial research for electric and PV cooling. Fluid flows in lateral confinements < 1 mm in micro heat exchangers. Microchannels with hydraulic diameters ≤ 1 mm is the most common confinement. In 1981, Tuckerman and Pease created microchannel heat sinks. Electronic component substrates in integrated circuits have several microchannels drilled into the back. Electronic components heat the coolant via forced convection [19].

Passive cooling systems using heat sinks

Numerous studies, experiments, and numerical simulations have been carried across the years to establish the optimal metal heat sink designs and applications for solar panels.
Passive cooling systems use convection, conduction, and radiation to move heat without energy. Since heatsinks have a longer lifespan, don't need external energy, and require minimum maintenance, passive cooling of PV modules is more investigated. In passive cooling, wind speed controls the convective heat transfer coefficient and PV temperature. Heatsinks lower PV module temperature by increasing heat rejection surface area.

Hetsroni et al. [20] tested constant temperature heat sinks for cooling. Two-phase cooling was used in this investigation. Comparing dielectric liquid and water cooling, Dielectric liquid had a maximum difference of 4–5°C and water cooling 20°C and reduced streamwise and transverse temperature gradients. Min et al. [21] tested $400 \times$ PV metal heat sinks outdoors. The study examined how temperature affected cell regions with different concentration ratios. Heat sinks needed to be 700 times larger than solar cells to maintain a 37 °C average temperature.

Gotmare et al. [22] experimentally tested a passively cooled PV module. Different porous aluminum fin designs were tested on a 37 W/0.351 m^2 PV module. Aluminum (Al) fins reduced module temperature by 4.6% and increased output by 5.5% compared to the reference PV module. This study evaluated several heatsinks, but no computational analysis was done. Cuce et al. [23] tested passively cooled polycrystalline PV cells with an aluminum heatsink. A custom solar simulator increased 10% energy efficiency, 20% exergy efficiency and power conversion 13%, solar irradiation for this case was 800 W/m^2. PV module cooling was minimal at 200 W/m^2 and maximal at 600 W/m^2. Chen et al. [24] tested polycrystalline PV module cooling. To study the way temperature, inclination, irradiation, and velocity affect efficiency and power production, a passive cooling solution was used. The PV module with 0.8 mm aluminum alloy fins was compared to the base PV module. Ambient temperature decreases electrical efficiency and power output. Fins enhanced power production by 1.8% and electrical efficiency by 0.3%. With PV module orientation, electrical efficiency fell first and climbed progressively. Power output behaved otherwise. Passive cooling in this experiment enhanced average electrical efficiency by 1.3% and power production by 3.1%.

Soliman et al. [25] investigated PV cell cooling with aluminum heat spreaders. To lower the temperature of the 125 mm X 125 mm PV cell, the aluminum plate's optimal size was found to be 0.3 m^2 area and 10 mm thick. Compared to the reference configuration, efficiency and output power increased by 9% and 15 °C. Due to material weight, space limits, etc., the suggested aluminum plate dimensions for appropriate cooling may change from a full-scale PV module. Kim and Nam [26] computed passive cooling using fins with and without slits. The reference setup had 13.24% efficiency and 62.78 °C surface temperature. Fin-passive cooling increased efficiency by 7.96% and lowered the temperature by 15 °C. A slit reduced temperature by 8.62 °C. Triangular fins have sharp edges and cutting slots that can make heatsink production more expensive.

Bayrak et al. [27] examined how fin shapes affected the cooling efficiency and temperature of a 75 W polycrystalline module which examined ten combinations. The maximum energy and exergy efficiencies were 11.6% and 11% for each example. Optimal arrangement has 772.83 W/m2 and a maximum 3.39 °C temperature difference from the base case. Hasan [28] tested the cooling of the heatsink with a 10 W polycrystalline module of 0.09975 m^2. The heatsink that was used had a trapezoidal fin profile with a base plate. Power output increased by 15.3% and module temperature decreased by 5.7 °C. Marco Tina [29] created an analytical model to study how PV module temperature distribution affects electrical behavior. The study found shadow to be one of the main causes of uneven module temperature and suggested using PV cooling to fix the issue.

One of the most recent analytical works on passive cooling solutions for PV panels, by Haque et al. [8], in which 19 distinct configurations of three different aluminum heatsinks were studied to determine their effectiveness. At 35°C, 800 W/m^2, and 10 W/m^{2}K of convective heat transfer, a combination type heat sink consisting of a flat base and fins with small openings achieved the best results, reducing the PV panel temperature to 56.23°C as opposed to 73.84°C for a base panel.

The literature included above exhibits numerous heatsink solutions for PV panels of varying dimensions, with most studies focusing on heatsink-based PV cooling. When compared to alternative methods of PV cooling, reducing the module temperature using just heatsinks offers certain basic advantages in terms of consistency and achieving the highest possible level of performance. The purpose of this research is to give an experimental analysis of a heatsink configuration with an aluminum base plate and fins fitted in polycrystalline PV modules concerning PV temperature, and heat dissipation area.

Section 2.4 Identification of the heat sink model

In a solar panel, heat dissipation is crucial for maximizing the efficiency and durability of the panel. Using a heat absorber is a common method for controlling the temperature of the panel. The purpose of a heat sink is to transfer heat from a heated object to a cooler object. Typically, heat sinks are constructed from materials with high thermal conductivity, such as aluminum or copper. When selecting a heat absorber for a solar panel, several factors must be considered. The factors include material consumption, fin size, aluminum weight, and numerical analysis derived from a previous review of the literature.

Material consumption is an essential consideration when choosing a heat absorber. The production cost and total weight of a panel can be impacted by the quantity of material used in the heat sink. Therefore, it is essential to choose a heat sink that utilizes the smallest amount of material required for efficient heat dissipation.

The size of the fins is another essential consideration when selecting a heat sink. The fin size can impact the heat sink's ability to dissipate heat. A larger fin dimension can increase the heat dissipation capacity of the heat sink but can also increase its weight and cost. Therefore, choosing a fin size suitable for the solar panel model is essential.

The weight of the aluminum must also be considered when selecting a heat absorber. The heat sink's weight can affect the solar panel's total weight, which can affect the panel's installation and transport. Therefore, it is essential to choose a heat sink that is both lightweight and effective at dissipating heat.

Haque et al. [8] recently conducted an analysis of the effectiveness of passive cooling solutions for PV panels. The study involved evaluating the efficacy of 19 distinct configurations of three types of aluminum heat sinks under specific conditions. Conditions included 800 W/m2 of irradiance, 35°C of temperature, and a convective heat transfer coefficient of 10 W/m2K.

The study found that a heat sink with a combination of a flat base and fins with small apertures reduced the PV panel's temperature the most effectively. The panel temperature was reduced to 56.23°C, which was substantially lower than the base panel temperature of 73.84°C. The perforated heat sink with perforations outperformed all other tested configurations.

To enhance the testing process for heat sinks, a simulation method can be employed and then validated through experimentation, or vice versa. Arifin et al. [30] conducted research using a simulation technique, followed by experimental research involving the use of a perforated aluminum heat sink. The purpose of the holes in the fins was to enhance the efficiency of the heat sink by increasing the natural convection airflow release.

Due to their high thermal conductivity, copper and aluminum are commonly used for heat sinks. Copper has a higher thermal conductivity than aluminum, meaning that heat transfer occurs more rapidly in copper than in aluminum. In order to expedite the heat transfer process, heat sinks are typically equipped with perforated fins that permit the wind to travel through and release the heat into the surrounding environment.

When selecting a heat absorber for a model solar panel, it is vital to consider these findings. It is

crucial to select a material with high thermal conductivity, and the use of perforated fins can considerably enhance the heat sink's performance. The research of Arifin et al. demonstrates the importance of integrating simulation and experimentation to optimize heat sink design and enhance their performance.

Another study by Elbreki et al. [31] examined the effectiveness of passive cooling for concentrated photovoltaic modules using two inventive designs of passive fin heat sinks, namely overlapping and longitudinal fins. Utilizing the Design of Experiment (DOE) approach, the optimal design parameters were determined by analyzing the fin height, fin pitch, fin thickness, number of fins, and tilt angle. The experimental work was conducted under actual environmental conditions, with the optimal design parameters for passive fin heat sinks in place. The results indicate that the design with overlapping fins obtained the best performance, with a mean PV module temperature that was 24.6 °C lower than the PV module used as a reference. At an average solar irradiance of 1000 W/m2 and an ambient temperature of 33 °C, this resulted in a high electrical efficiency of 10.68% and power output of 37.1 W. The study demonstrates the viability of passive cooling with overlapping fins as a method for enhancing the performance of concentrated PV modules.

3. Materials used in the Study

Section 3.1 Modelling of Heat Sinks

The heat sink under investigation in our study was created through a meticulous process of experimental analysis, based on the knowledge acquired from our exhaustive literature review. During this analysis, we identified two distinct configurations that we regarded appropriate for our research objectives. Nonetheless, substantial modifications were made to these configurations because of empirical data.

Adjustments to the initial configurations were necessitated by the need to realign the heat sink model with real-world conditions and practical limitations. These modifications were crucial for enhancing the efficacy and efficiency of the heat sink's design overall. Consequently, the final configurations chosen for our study demonstrate the novelty and originality of our research.

In the subsequent sections of our paper, we provide comprehensive descriptions of the design and structure of the heat sink model used in our investigations. In addition, we discuss the numerous parts and components that comprise the analysis setup. This exhaustive documentation

allows readers to acquire a thorough understanding of the experimental setup and methodology used in our study, thereby facilitating the replication and validation of our findings.

Sub Section 3.1.1 Heat Sink with Perforated Fins

It has been discovered that heat sinks with perforated fins offer several advantages over conventional heat sink designs. These advantages include enhanced thermal performance, weight reduction, and enhanced energy efficiency.

One of the most significant benefits of perforated fins is their capacity to increase the heat sink's surface area, thereby enhancing heat dissipation. The fins' holes also facilitate the release of natural convection wind, which increases the cooling effect. These advantages result in a decrease in the overall temperature of the solar panel, which can increase its efficiency and lifespan.

Another advantage of perforated fins is that they can reduce the heat sink's weight, which can be particularly useful in applications where weight is an issue, such as portable solar panels. This weight reduction can also result in material and transportation cost savings.

Additionally, the use of perforated fins can improve energy efficiency by decreasing the refrigeration system's power consumption. This is because the enhanced thermal performance of the heat sink reduces the need for energy-intensive active cooling methods, such as fans or pumps.
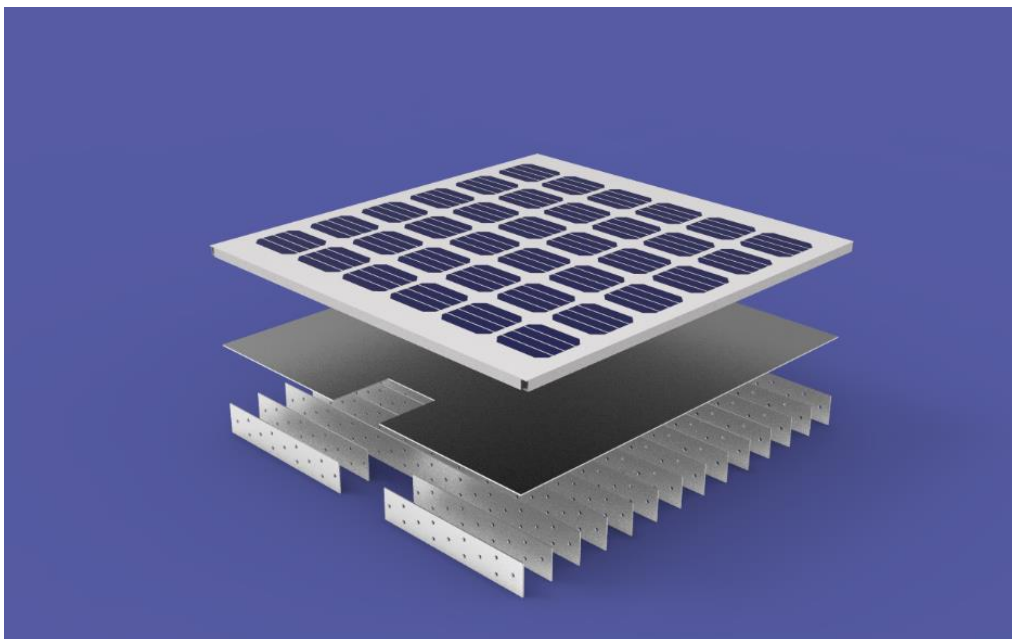

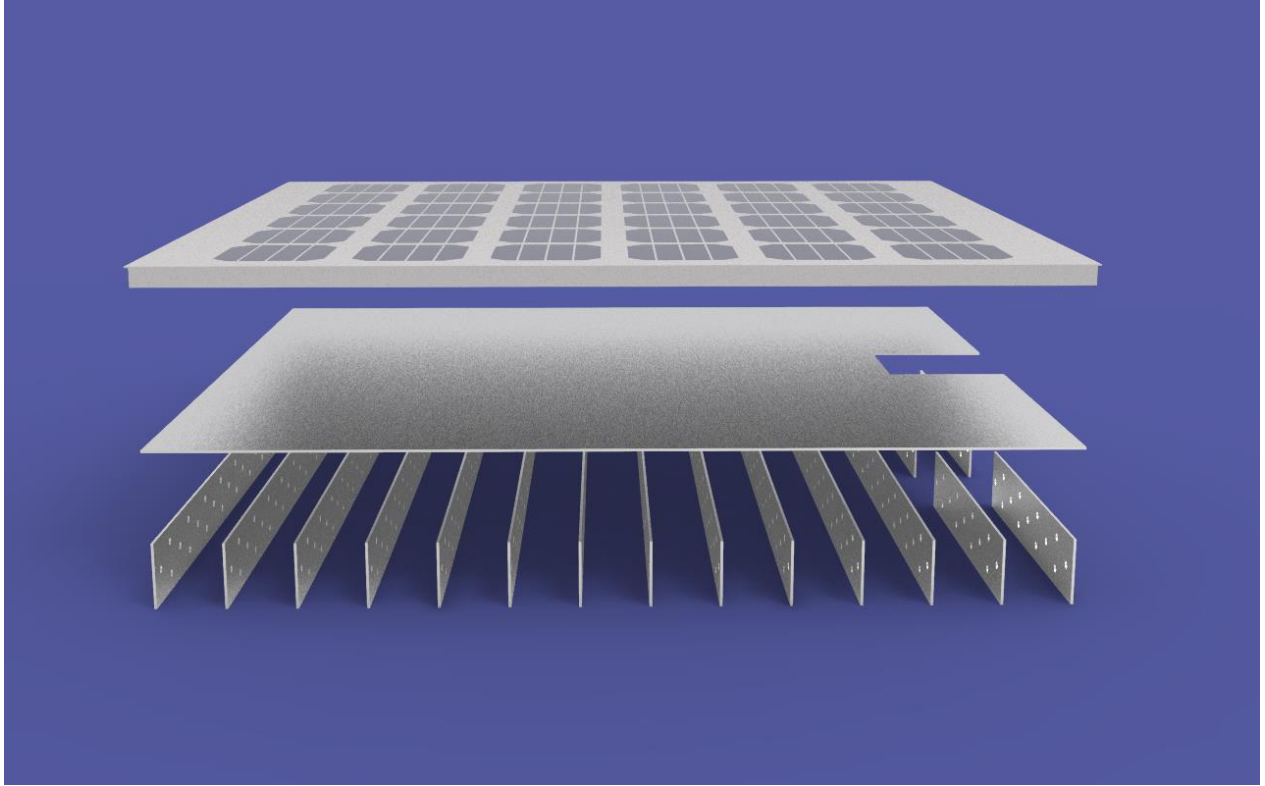*Figure 1Solar panel with perforated fin view 1*
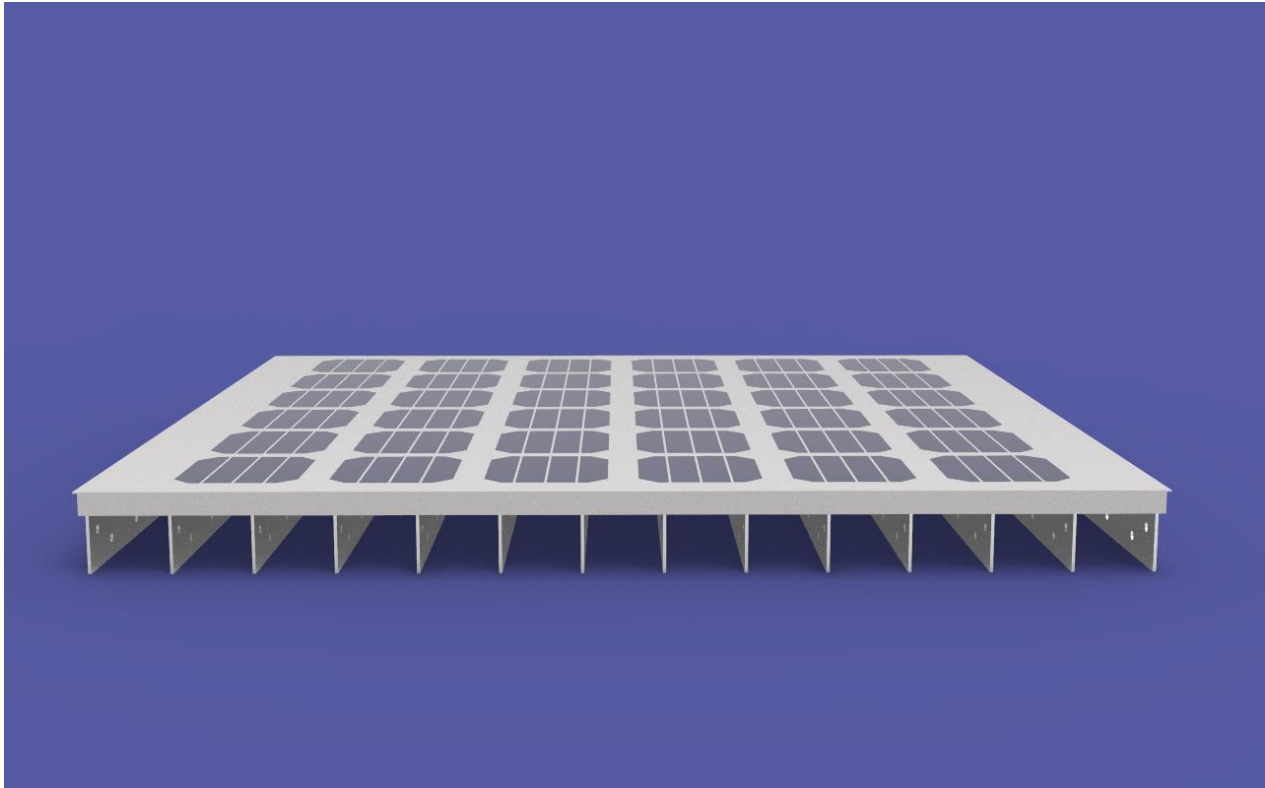
Figure 2 Solar Panel with perforated fin 2 view 2

Figure 3 Solar Panel with perforated fin view 3

Sub Section 3.1.2 Heat Sink with Plain fins

Heat sinks with conventional fins have been utilized for many years and continue to be popular due to their efficiency, dependability, and ease of manufacture. There are several advantages to using heat sinks with conventional fins rather than perforated fins.

One of the primary advantages of simple fin heat sinks is their capacity to provide a large surface area for efficient heat dissipation. Fins improve cooling performance by increasing the surface area for heat transmission by increasing the area in contact with the air. This increased surface area can assist in lowering the temperature of the solar panel, thereby enhancing its efficacy and extending its lifespan.

A further advantage of using heat sinks with conventional fins is that they are straightforward to manufacture. The fins can be produced by extrusion, stamping, or bonding, making them a cost-effective option. In addition, conventional fin heat sinks are available in a variety of sizes and configurations, allowing for greater design and application flexibility.

Likewise, heat sinks with basic fins offer a robust and reliable cooling solution. Typically, the fins are fabricated from superior thermally conducting materials, such as aluminum or copper. This conductivity allows for the rapid transfer of heat from the solar panel to the heat sink and subsequent dissipation into the environment. Simple fin heat sinks are frequently used in situations where failure cannot occur because of their dependability.
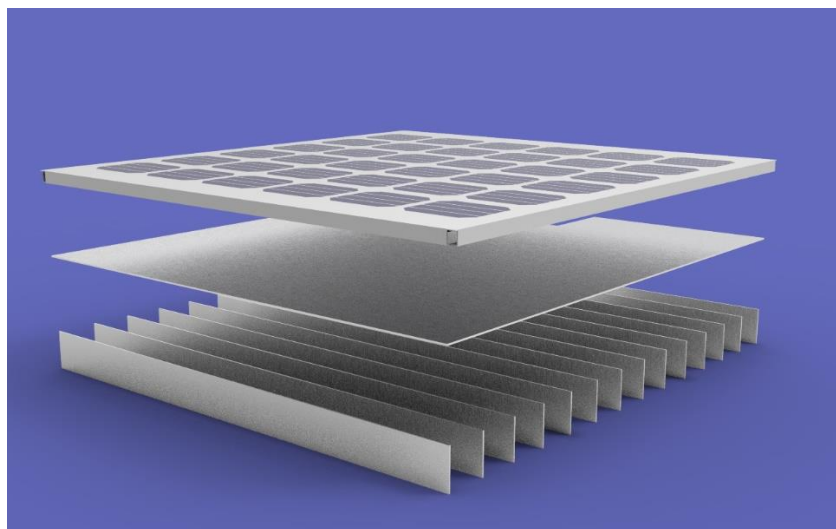

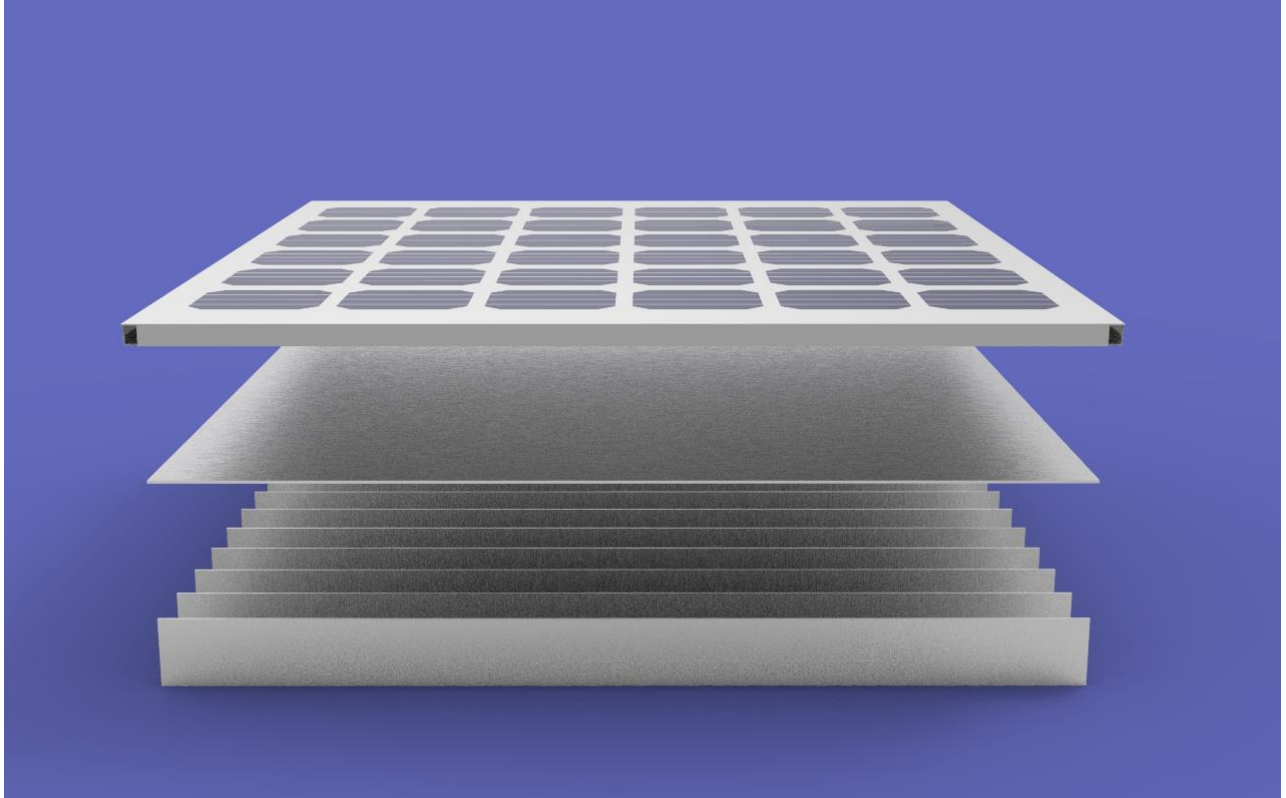*Figure 4 Solar panel with plain fin view 1*
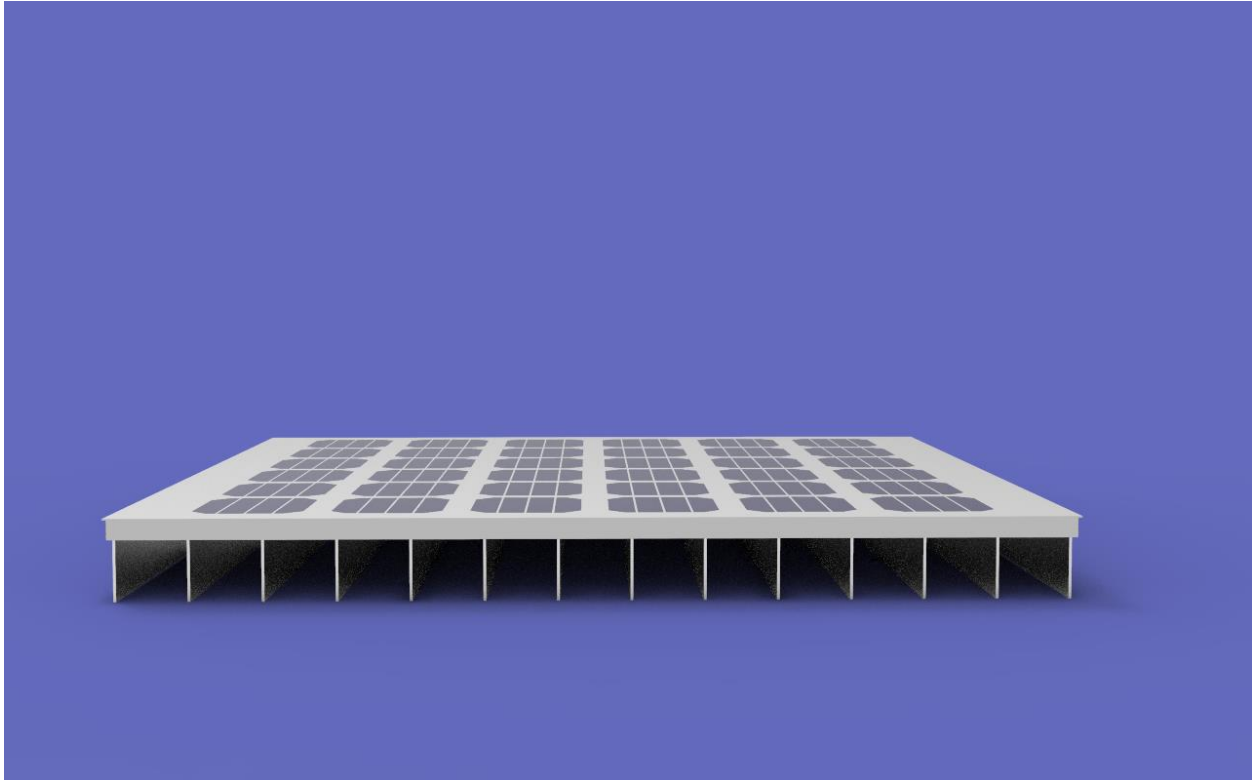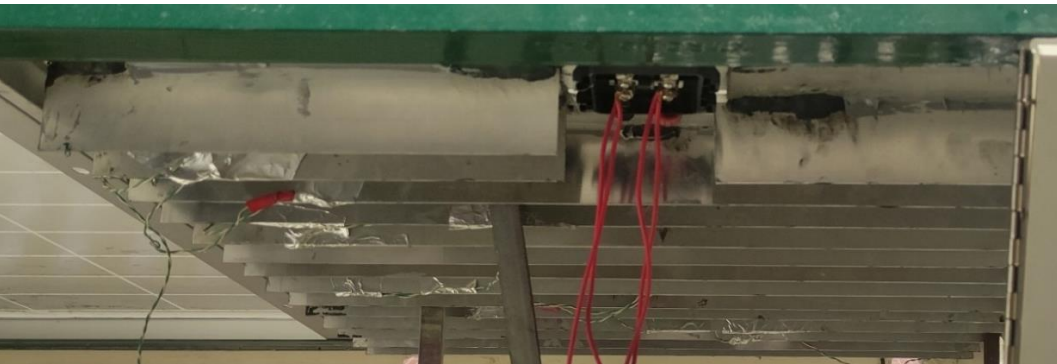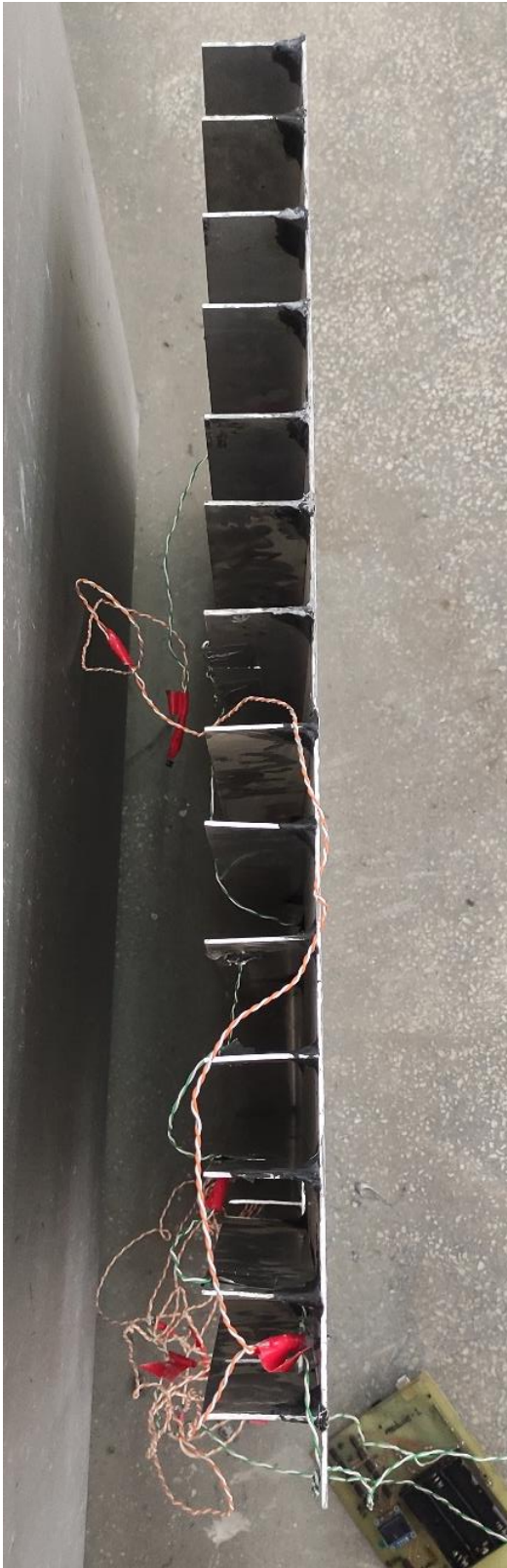
Figure 5 Solar panel with plain fin view 2

Figure 6 Solar panel with plain fin view 3

Section 3.2 Heat sink fabrication

The fabrication of heat absorbers is a crucial aspect of the design and construction of solar panels. Numerous techniques have been developed in recent years to improve the efficacy and effectiveness of heat sink fabrication, such as the use of Mseal resin to attach solar panel fins.

Mseal resin is a two-component epoxy adhesive utilized frequently in construction and engineering due to its high strength and durability. Mseal resin is used to attach fins to the solar panel in the fabrication of heat sinks, which increases the surface area available for heat transfer and aides in the more efficient dissipation of heat.

Concerns regarding the use of Mseal resin in the fabrication of heat sinks include the prospect that it will decrease the thermal conductivity of the heat sink, thereby diminishing its effectiveness. However, this can be mitigated by carefully applying the mseal resin. In this study, the mseal resin was applied only to the sidewalls of the fins and not to the contact point between the fin and solar panel. This method assured that the thermal conductivity of the heat sink was not compromised.

To maintain the connection between the fin and the solar panel, thermal paste was applied to the junction between the fin and the solar panel. This thermal paste is a high-thermal-conductivity material that occupies any gaps between the fin and the panel, thereby creating a low-resistance path for heat to travel from the solar panel to the heat sink. This procedure ensures that the heat sink is effective at dissipating heat and maintaining the solar panel's optimal temperature.

In conclusion, the use of Mseal resin in heat sink fabrication can be an effective means for attaching fins to a solar panel, thereby increasing the available surface area for heat transfer and enhancing the efficiency of the panel. By carefully applying the Mseal resin and utilizing thermal paste to maintain fin contact, it is possible to prevent any reduction in the heat sink's thermal conductivity and ensure its proper operation.
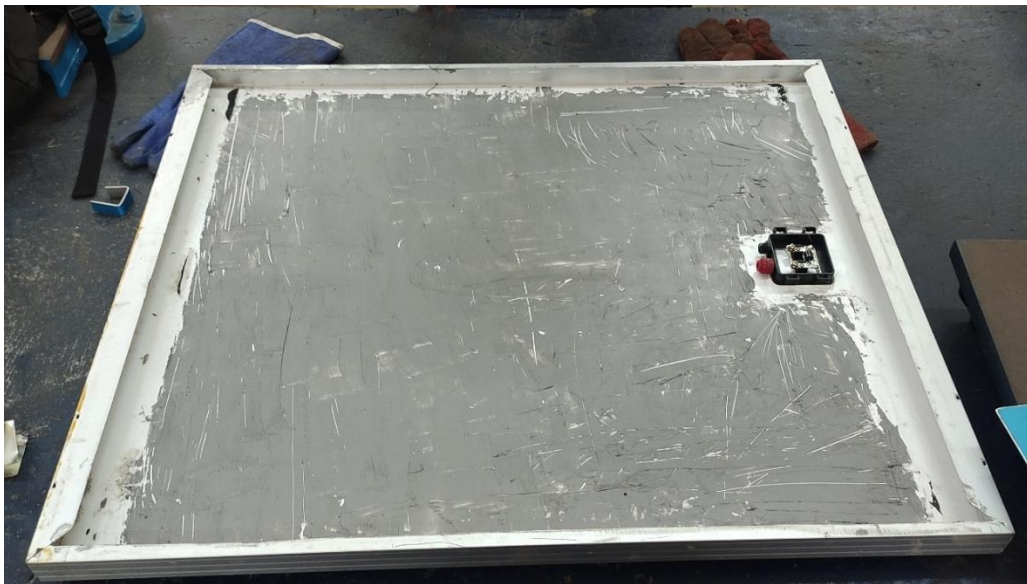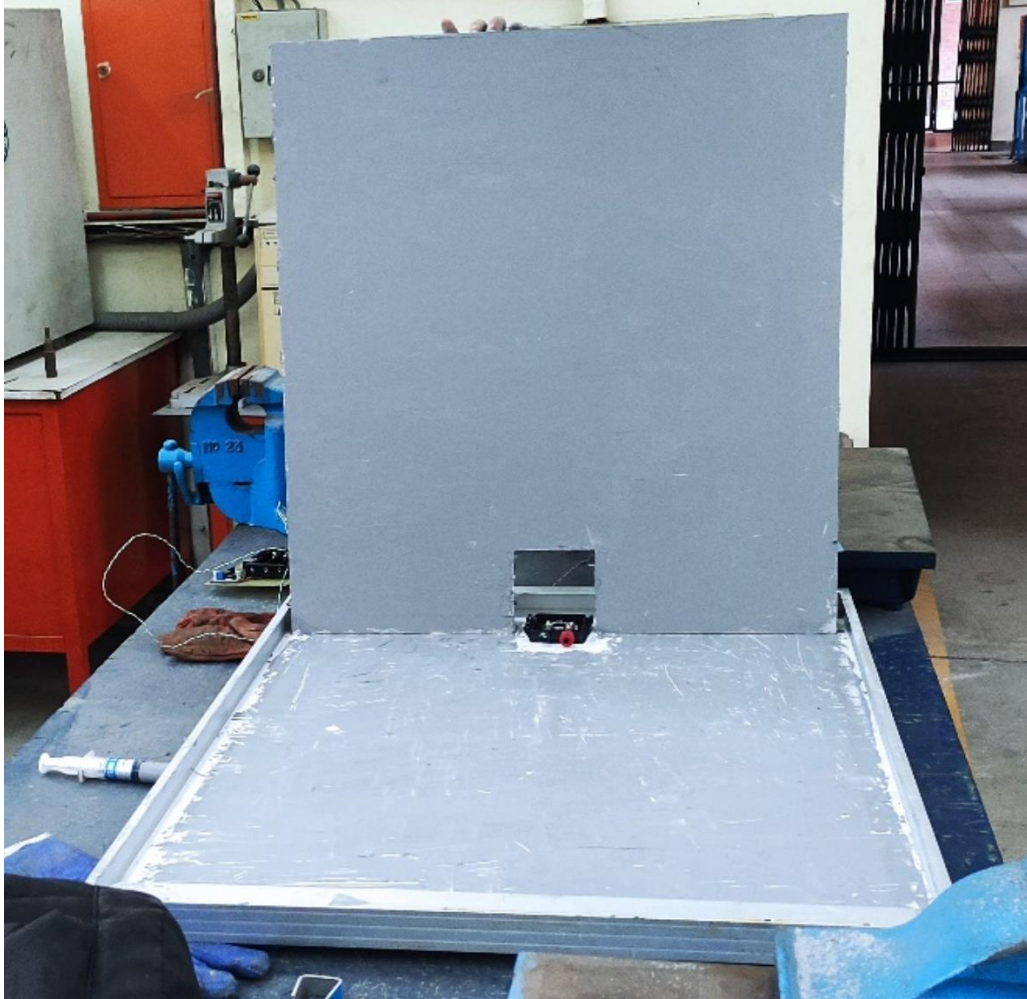
Section 3.3 Solar panel selection

Monocrystalline solar panels are among the most common types of solar panels utilized in residential and commercial environments. This is due to the fact that monocrystalline panels have several advantages over polycrystalline and thin-film solar panels.

The increased efficiency of monocrystalline solar panels is one of their primary advantages. Monocrystalline panels are manufactured from a single silicon crystal, so their cells are composed of a single, pure silicon crystal. This enables monocrystalline panels to have a higher efficiency rating, typically between 18% and 22%, than other panel varieties, whose efficiencies range from 15% to 17%.

Furthermore, the reduced size of monocrystalline solar panels is advantageous. Monocrystalline panels can generate the same amount of electricity as other varieties, but in a smaller area. This makes them a popular option for residential installations with limited space.

In addition to having a longer longevity than other solar panel types, monocrystalline panels typically have a minimum 25-year lifespan. This is due to the fact that they are constructed from superior materials and are less susceptible to deterioration over time.

Monocrystalline solar panels have several advantages over other types, including greater efficiency, smaller size, a longer longevity, and a more uniform appearance. This makes them a popular choice for an extensive range of applications, from residential rooftop installations to large-scale commercial projects.

Section 3.4 Configuring the Data acquisition System

Sub Section 3.4.1 Sensors Used in this study

The 0-25V DC voltage sensor is calibrated by making the necessary adjustments to ensure accurate voltage measurements within the range specified. This usually involves applying a series of voltages to the sensor and comparing its output to a known voltage source, such as a precise voltage reference. The calibration parameters of the sensor are modified based on any deviations between the output of the sensor and the known voltage. The procedure is frequently repeated multiple times to ensure that the sensor is calibrated accurately across its entire spectrum. In addition, software is utilized to calibrate the sensor by comparing its output to a known voltage source and

adjusting the resistor values within the sensor to match the known voltage.

A calibrated current sensor, such as the ACS 712 (30A), measures the current passing through it with great accuracy. Initial measurement involves a known current in the presence of a load. The current is then measured with a multimeter. Errors are computed after outputs have been compared. Depending on the results, the gain or offset of the sensor is modified. Additionally, the internal amplifier's parameters are modified. This process is repeated repeatedly. Lastly, the performance of the sensor is validated by measuring the current traveling through the sensor under different load conditions to ensure the sensor's accuracy under a variety of conditions.

Current sensor

The Model AC3712 30A is a completely integrated, Hall effect-based linear current sensor. Using its integrated low-resistance current conductor, this device can precisely measure the amount of current applied and provides a voltage isolation of 2.1kVRMS.

In technical terms, the ACS712 uses its conductor to calculate and measure current, as well as to provide a low-noise analog signal path. The device's bandwidth is set via the new FILTER port, and its output sensitivity ranges from 66 to 185 mV/A with an 80kHz bandwidth.

In addition, the ACS712 has an internal conductor resistance of 1.2 m, a stable output offset voltage, and magnetic hysteresis that is close to zero. At TA = 25°C, its total output error is 1.5%, making it a reliable and accurate current sensor.
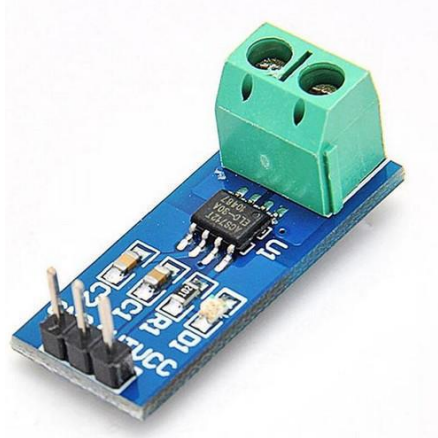

Figure 7 Current sensor

Temperature sensor

The DS18B20 is a programmable digital temperature sensor that provides temperature readings with a resolution of up to 0.0625°C. Typically, the manufacturer specifies the accuracy of the

sensor as 0.5°C over the temperature range of -10°C to +85°C.

This sensor has a power supply range of 3.0V to 5.5V and can communicate via the 1-Wire protocol. -67°F to +257°F is the Fahrenheit temperature range that can be displayed for temperature readings. The output resolution can range from 9 bits to 12 bits, and the sensor can convert a 12-bit temperature reading into a digital word in less than 750 milliseconds.

The DS18B20 is energized via the data line and features programmable alarm options. Additionally, its unique 64-bit address facilitates multiplexing. This sensor has a temperature range of -55°C to +125°C and is offered in a variety of packaging options, including SOP, To-92, and impermeable.

Figure 8 Temperature sensor

Voltage Sensor

The Voltage Sensor Module is a simple yet incredibly useful module that uses a potential divider to reduce the input voltage by a factor of 5. This module, specifically the 0-25V Voltage Sensor Module, enables monitoring of voltages greater than what a microcontroller's analog input can typically detect.

This sensor has an analog output, an input voltage ranges from 0 to 25V, and a voltage detection range from 0.02445V to 25V. The analog voltage resolution is 0.00489V, and the module measures 4 by 3 by 2 centimeters. The manufacturer specifies that the error rate for this Voltage Sensor Module is 1%, ensuring accurate voltage monitoring.

Figure 9 Voltage sensor

Irradiance Sensor

The H1750FVI is a digital light sensor with an I2C bus interface, which makes it an ideal ambient light sensor IC for adjusting the LCD and keypad backlight output of mobile phones. This sensor's ability to detect a broad spectrum at a high resolution (1 - 65535 lx) makes it a highly reliable source of ambient light data. The ability of this sensor's illuminance-to-digital converter to convert illuminance into digital data is one of its chief advantages. It also has a low current consumption thanks to its power-down feature and can reject 50Hz/60Hz light pollution. In addition, the H1750FVI has an I2C bus interface that supports f/s mode, allowing for simple integration into a variety of systems without the need for additional components.

Figure 10 Irradiance sensor

Data logging systems

To successfully carry out the experiment, it is necessary to continuously log data. Data regarding voltage, current, and temperature were all logged for both panels throughout the day. The use of light sensors allowed for the logging of irradiance data as well. The 26 Arduino-based microcontrollers were used to construct data logging systems. The data of the temperatures taken at 14 distinct places were logged

Section 3.5 Temperature Logging Systems

The purpose of developing this system was to log temperature data on ten distinct spots of the PV module that was integrated with the heat sink. The temperature of the PV was logged once every two minutes. That would be 0.0083 hertz for the frequency at that this data logger system was operating. Table 6 List of components used to develop data Logger 1.

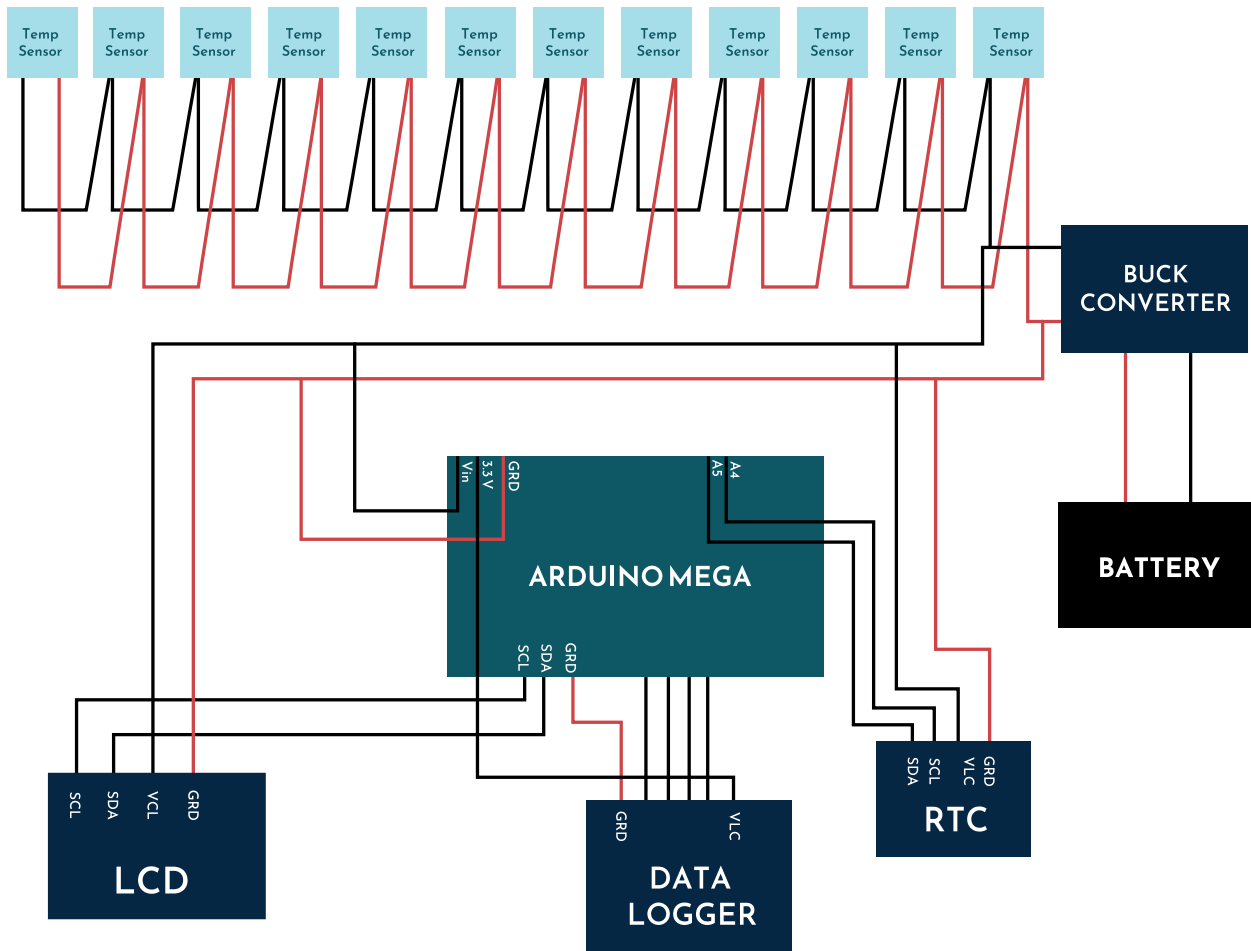| Components	Model	Quantity
Microcontroller	Arduino Mega 2560 Rev3	02
Temperature sensor	DS18B20	12
Real Time Clock (RTC)	RTC DS3231 – EEPROM MODULE	01
Display	0.96 OLED Display	01
Buck Converter	DC converter with voltage regulator	01
Battery	18650 - 3.7 V – 3800 mAh	03
SD card module	SD Card <=2G, SDHC card (<=32G)	01

Figure 11 Temperature logging system

Section 3.6 Current and Voltage Logging Systems

This data logger based on Arduino was utilized so that the data for irradiance, current, and voltage could be logged. This device operates at a frequency of 0.0083 hertz. That is, it creates a log after each interval of 2 minutes. Table 8 List of components used to develop data logger 1.

Components	Model	Quantity
Microcontroller	Arduino Nano	01
Voltage sensor	DC 0-25V	02
Real Time Clock (RTC)	RTC DS3231 – EEPROM MODULE	01
Current Sensor	AC3712 30A	01
Light intensity Sensor	BH1750	01
Battery	18650 - 3.7 V – 3800 mAh	03
SD card module	SD Card <=2G, SDHC card (<=32G)	01
Buck Converter	DC converter with voltage regulator	01

Figure 12 Voltage and Current logging system
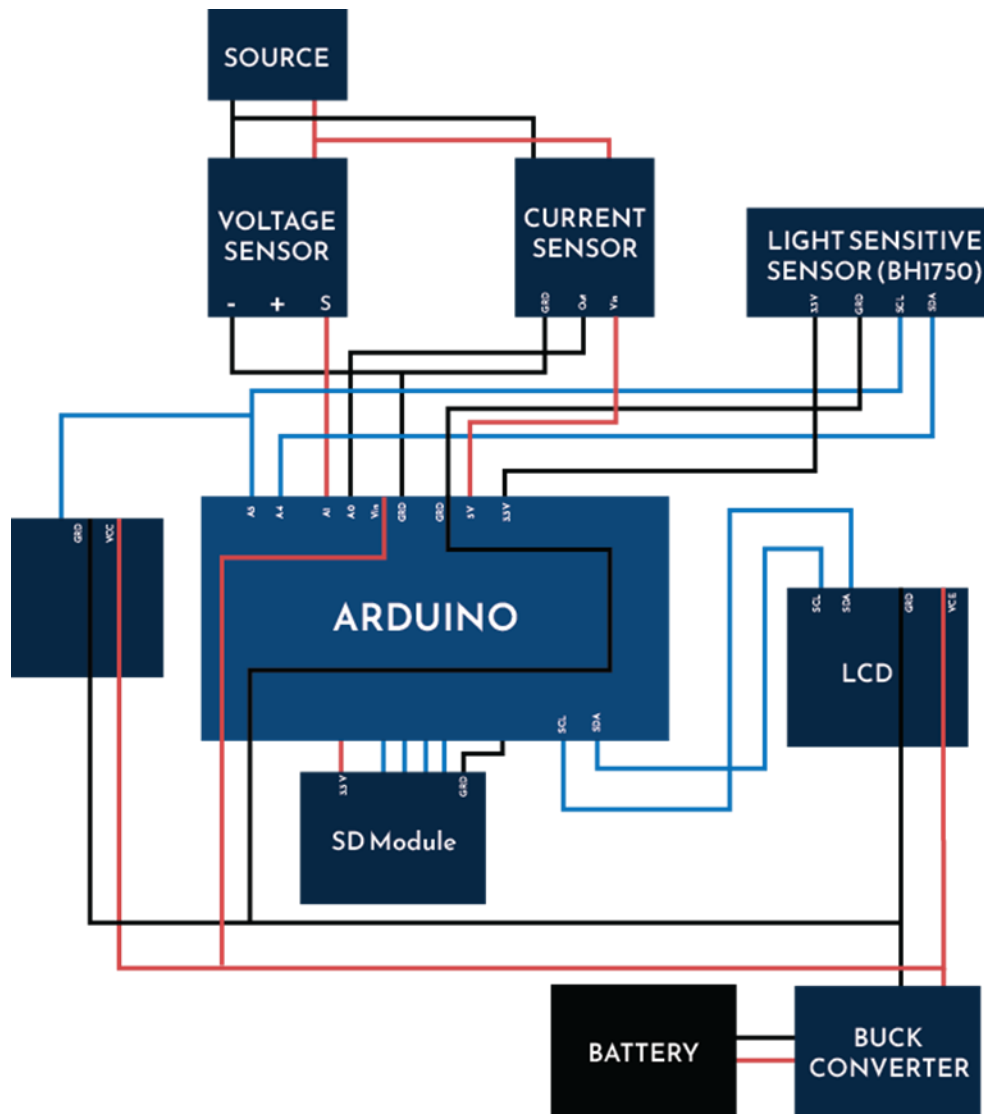
4. Methodology

This section describes the methodology that was utilized in the study we conducted. The numerical setup, a description of the heat sink's configuration, and a description of the data recording systems as well as their constituent components are listed. Here are listed all the governing parameters that were required for or considered when conducting the experiment.

Section 4.1 Numerical setup

The aluminum heat sink was attached to the rear of a vertical solar panel, which had perforations drilled into its fins to increase airflow and hence heat absorption. The modeling software operated under the assumption that the PV panel was a discrete composite layer.

Each layer of the solar module and its characteristics are listed in the following table. It is assumed that these layers' properties are invariant under both temperature and pressure.

PV Layer	Density (kg/m3)	Specific heat capacity(kj/kgK)	Thermal conductivity(W/m K)	Thickness (mm)
Glass	2450	0.79	0.7	3.2
EVA	960	2.09	0.311	0.5
PV cell	2330	0.677	130	0.21
EVA	960	2.09	0.311	0.5
PVF	1200	1.25	0.15	0.3

The average temperature and wind speed in Bangladesh is 35 degrees Celsius and 1.5 meters per second (m/s), respectively. The Reynolds number (Re) and turbulence intensity (I) were determined using the equations below.

$$\text{Re} = \frac{\rho V D}{\mu}$$

$$I = 0.16\text{Re}^{-1/8}$$

where ρ and μ represent the fluid's density (kg/m3) and viscosity (kg/ms), respectively. The necessary air velocity was calculated to be around 13100 Reynolds number, with an anticipated turbulence intensity of 4.8%.

The PV panel was subjected to 1000W/m2 of solar radiation under standard test conditions, and this radiation was converted into electrical energy via the PV effects mechanism. Tempered glass reflects between 3 and 10% of the solar radiation to the cell's surroundings, while crystalline silicon solar cells have an electrical efficiency between 11 and 20%. The researchers assumed that the solar module converts just 25% of the sun's energy into electricity before reflecting the rest back into the atmosphere.

Section 4.2 Experimental Setup

Sub Section 4.2.1 Setup of Solar PV panel

To carry out the experiment, two distinct solar modules with precisely the same setup were utilized. Comparison research was carried out using two identical panels, one of which had a heat sink built into it, while the other panel was left without a heat sink. For the experimental analysis, two monocrystalline solar panels were utilized. Since a comparison analysis was performed, the results of the experiment will not be affected in any way by this. The use of monocrystalline solar panels was decided upon for the following reasons: Monocrystalline cells have a higher efficiency. The temperature coefficient of monocrystalline cells is lower than that of polycrystalline cells. When the temperature rises by one-degree, monocrystalline solar panels experience a loss of power production capability equal to 0.35% of their total capacity. This rate is 0.4% for every degree when it comes to polycrystalline panels. Bangladesh experiences an overall temperature of about 26⁰ Celsius. When the PV module temperature reaches approximately 55⁰ Celsius, the ability of polycrystalline panels to produce electricity is reduced by 12%, while the ability of monocrystalline cells to produce electricity is reduced by approximately 10%. Therefore, the performance of monocrystalline cells is superior in higher temperatures. Because of these factors, a monocrystalline solar PV panel was selected for the purpose of the experimental analysis. Because Gazipur, Bangladesh is located at a latitude of 23.59⁰, the panels are tilted at an angle of 23.60⁰. The entire solar module along with the testing apparatus was converted into a portable form. The system has wheels attached to it so that it can be moved to any location and the maximum amount of solar irradiance can be collected throughout the day. This strategy was implemented because of a scarcity of open unoccupied space as well as other structures.
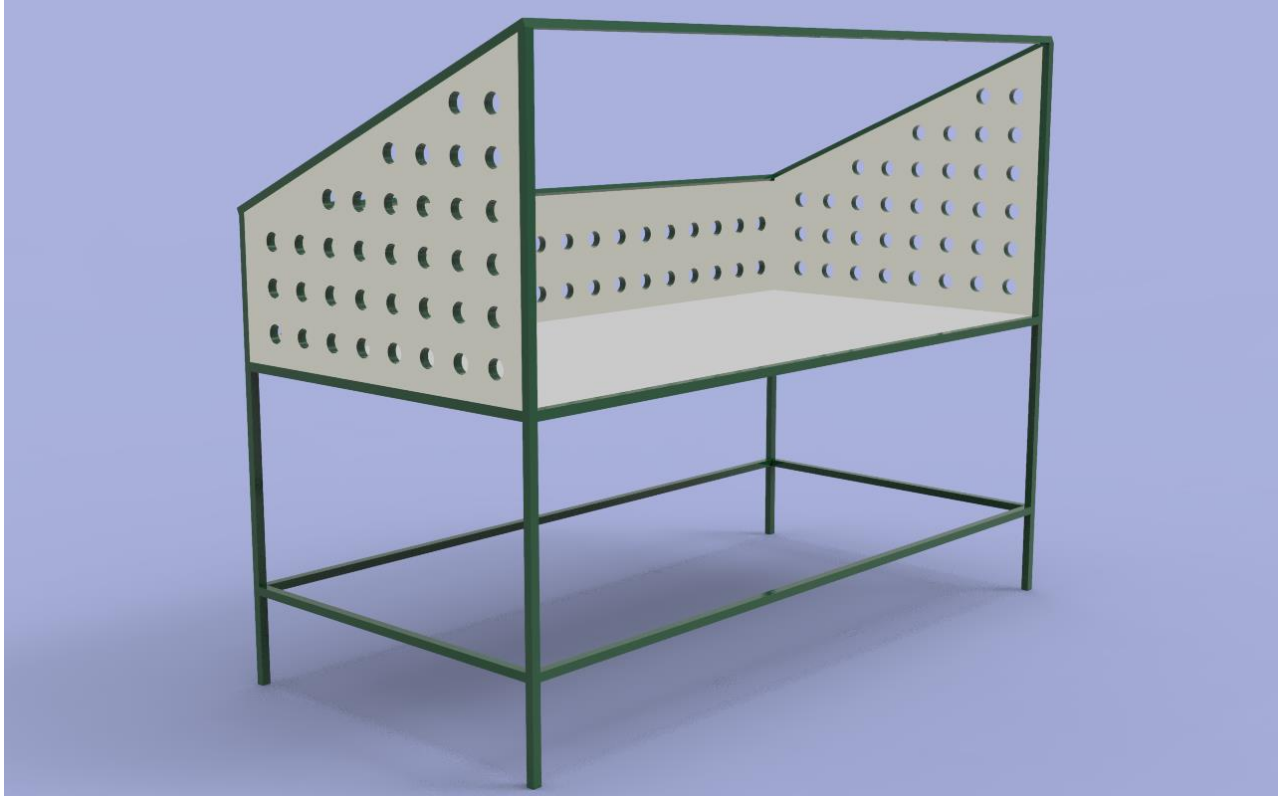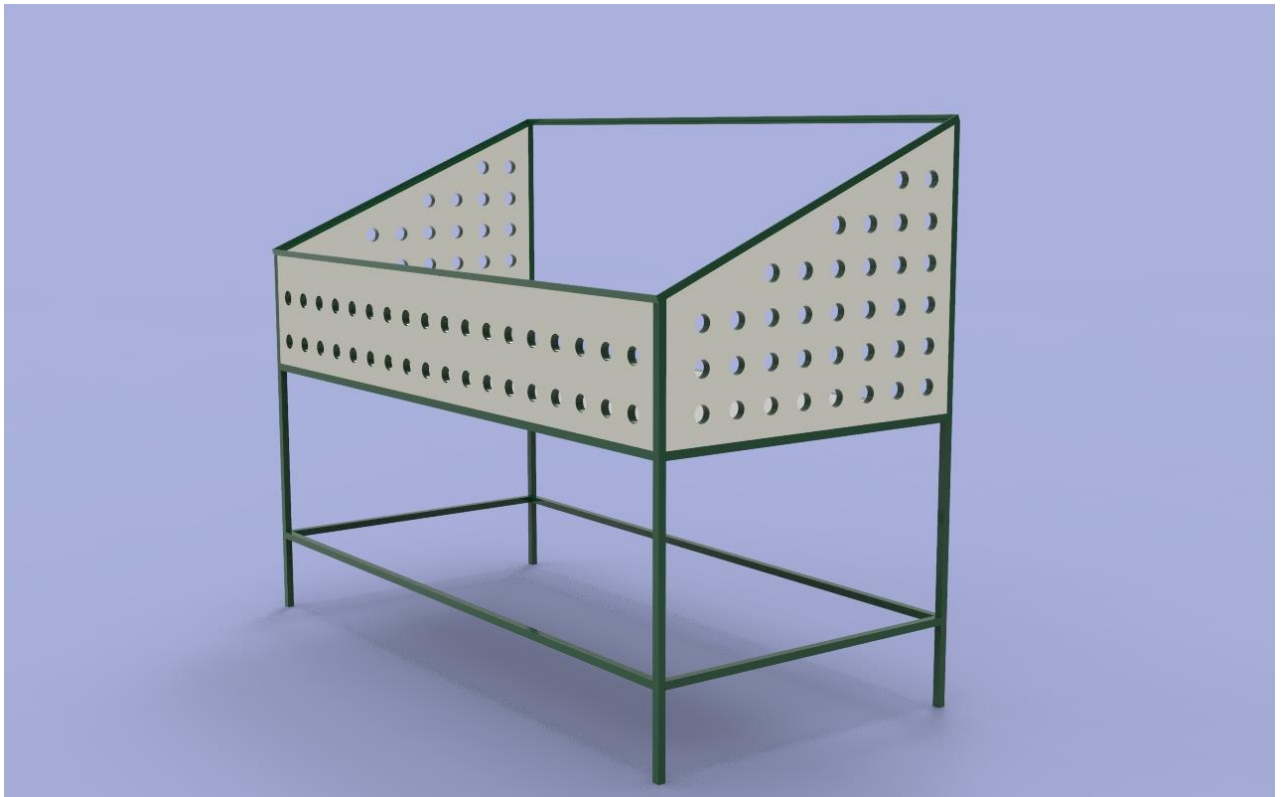
Figure 13 Frame view 1
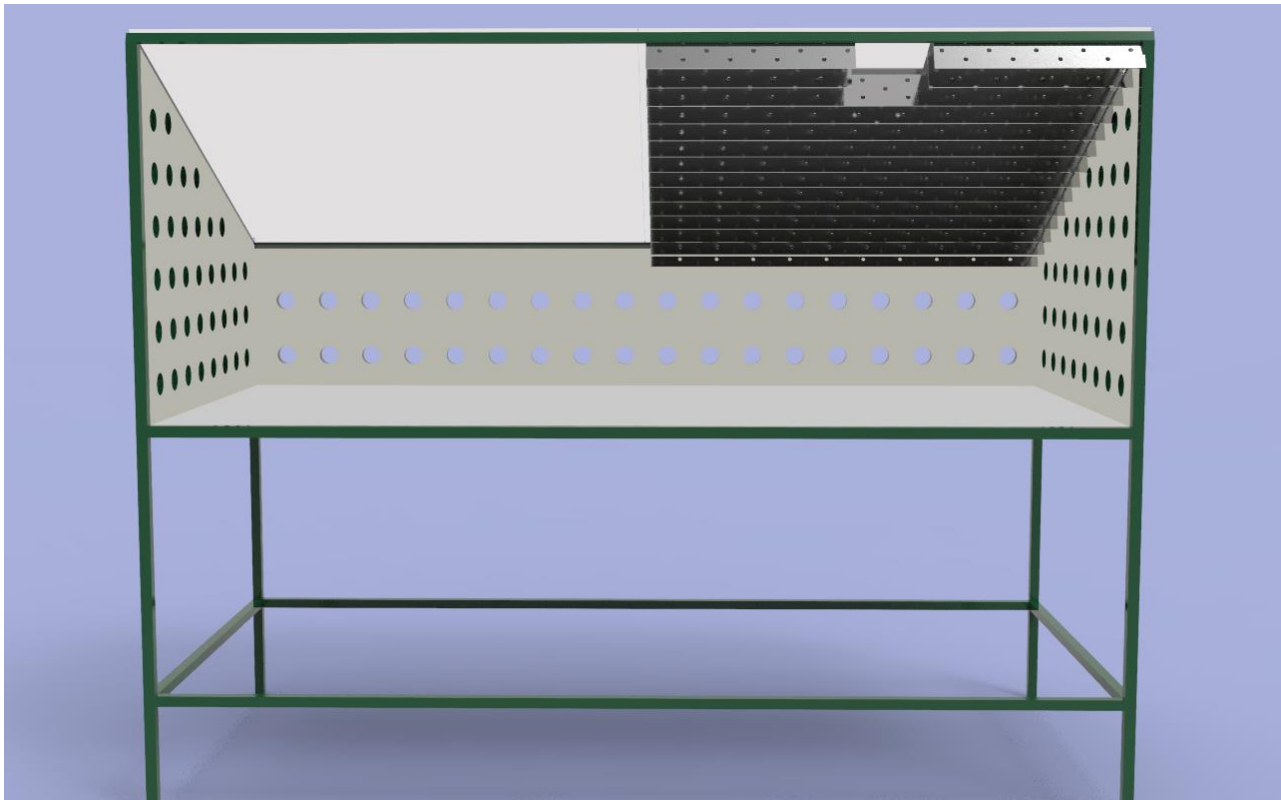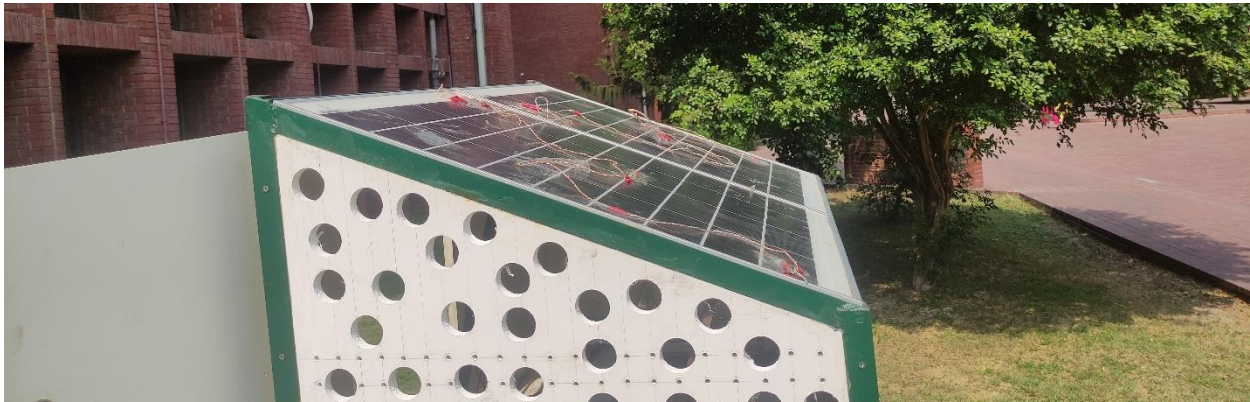

Figure 14 Frame view 2

Figure 15 Full setup

Figure 16 Full setup with Heatsink view

Sub Section 4.2.2 Solar Panel Characteristics

The solar panel used in this study is an 85 Wp (watt peak) mono crystalline module manufactured by PT Len Industries. The Grameen Power Industries 85 Wp solar panel module is detailed in Table 1, while the 85 Wp mono crystalline solar panels are depicted in Figure 1.

Features	value
Power Tolerancce	5%
Max. Power Voltage Vmp (V)	17
Max. Power Current Imp (A)	4.71
Open Circuit Voltage Voc (V)	22.18
Short Circuit Current Isc (A)	5.11
Max. System Voltage VDC	600
Pm Temperature Coefficient	-0.4
Isc Temperature Coefficient	4.7
Voc Temperature Coefficient	-2
NOCT- Nominal operating cell temp. (Celsius)	45

Sub Section 4.2.3 Solar Panel Calibration

Solar panel calibration is essential for ensuring the accuracy and reliability of measurements of solar panel performance. The standard procedure for solar panel calibration consists of the following steps:

During the initial step of solar panel calibration, the panel is prepared for testing. This may involve cleaning the panel, removing any dirt or detritus, and ensuring all connections are secure and operational.

Monitoring climatic conditions is the subsequent step. It is crucial to measure factors such as temperature, humidity, wind speed, and irradiance, as weather conditions can significantly impact

solar panel performance. This data can be used to account for variations in performance caused by meteorological conditions.

Next, it is necessary to measure the irradiance, or the amount of solar radiation reaching the panel. This can be accomplished using a pyranometer, which measures the intensity of incoming solar radiation.

The subsequent step entails measuring the panel's electrical output. This can be accomplished using a multimeter or other electrical measuring instrument. The output voltage, current, and power of the solar panel must be measured and recorded.

After taking measurements, the data should be analyzed to determine the panel's performance characteristics. This may involve calculating the solar panel's efficacy, power output, and other performance metrics.

The panel should be calibrated based on the outcomes of the data analysis. This may entail adjusting the panel's position or orientation, compensating for weather conditions, or making other performance-enhancing modifications.

Solar panel calibration is an ongoing process, and panels should be rechecked and recalibrated frequently to ensure that they are operating at peak efficiency. By adhering to a standardized procedure for solar panel calibration, the performance of solar panels can be precisely measured and optimized, leading to greater energy production and efficiency.

Sub Section 4.2.4 Sensor Calibration

Sensor Adjustment The 0-25V DC voltage sensor is calibrated by making the necessary adjustments to ensure accurate voltage measurements within the specified range. Typically, this requires applying a series of voltages to the sensor and comparing its output to a known voltage source, such as a precise voltage reference. Adjustments are made to the sensor's calibration parameters based on any deviations between the sensor's output and the known voltage. In order to ensure that the sensor is calibrated accurately across its entire spectrum, the procedure is frequently repeated multiple times. Software is also used to calibrate the sensor by comparing its output to a known voltage source and modifying the resistor values within the sensor to match the known voltage. A calibrated current sensor, such as the ACS 712 (30A), precisely measures the current traveling through it. In the presence of a burden, a known current is initially measured. Next, the same current is measured using a multimeter. After comparing outputs, errors are computed. Depending on the results, the sensor's gain or offset is adjusted. Additionally, the

parameters of the internal amplifier are modified. This procedure is repeated numerous times. Finally, the performance of the sensor is affirmed by measuring the current flowing through the sensor under various load conditions in order to ensure the sensor's accuracy under a variety of conditions.

Calibration of temperature sensors is essential for ensuring their accuracy and reliability. Using an oven or other temperature-controlled environment to establish a reference temperature for calibrating the sensors is one of the most common temperature calibration methods.

The standard procedure for temperature calibration involves multiple steps. Prior to calibration, the sensors are cleansed, sanitized, and examined to ensure that they are operating properly. The sensors are calibrated by placing them in an oven or other temperature-controlled environment that can provide a constant reference temperature.

The temperature is then incrementally increased until it reaches the desired calibration temperature, allowing the sensors to adapt to each new temperature level. Once the desired calibration temperature has been reached, the accuracy of the sensors is determined by comparing their output to a known reference temperature. Adjustments are made to the sensors as necessary to ensure that they remain within the tolerance range.

After sensors have been calibrated, they must be examined to ensure their accuracy and dependability. This may necessitate additional testing or investigation. The results of the calibration are then documented and stored for future reference, including the calibration procedures utilized, the reference temperature values, the sensor output values, and any sensor adjustments.

To ensure the accuracy and dependability of temperature sensors, it is necessary to follow a standard calibration procedure involving an oven or other temperature-controlled environment. Sensors can provide accurate temperature measurements for a variety of applications when precisely calibrated.

Sub Section 4.2.5 Procedure of Connecting the Temperature acquisitions of the solar panel

To analyze the thermal behavior of a solar panel with a built-in heat sink, we conducted an experiment in which temperature measurements were obtained at various locations on the module. Ten sensors were strategically placed across the panel to acquire a complete picture of the temperature distribution.

Two of the temperature sensors were affixed to the heat sink's fins to monitor the temperature at specific points along the heat dissipation path. In addition, four sensors were affixed to the heat sink's base plate in order to measure the temperature at various nearby locations. Additionally, three temperature sensors were installed on the active area of the module's upper surface to measure the temperature at various locations.

We utilized a dependable method of sensor attachment to guarantee accurate temperature readings. Thermal paste was applied beneath the aluminum foil tape to eradicate any air gaps between the sensor and the measuring surface. This method assured optimal thermal contact and reduced any potential heat transfer impediments.

In addition, we gathered temperature information from the three areas of the solar panel that lacked a heat absorber. These sensors were diagonally positioned on the panel to capture temperature readings from various regions. These sensors were affixed utilizing the same procedure as the heat sink-integrated sensors.

For the long-term collection of temperature data, an Arduino-based data recorder was utilized. From 8:00 a.m. to 6:00 p.m., this device was programmed to record temperature readings every two minutes. As the solar panel was portable, we positioned it in the most advantageous location to maximize solar irradiance and ensure realistic operating conditions throughout the experiment.

Using this exhaustive experimental configuration, we intended to collect precise temperature data and gain insight into the thermal performance of the heat sink-integrated solar panel. The collected data would be beneficial for evaluating the heat sink's ability to regulate temperature and enhance the solar panel's overall performance.

Figure 17 Experimental setup view 1

Figure 18 Experimental setup view 2

Figure 19 Experimental setup view 3

Figure 20 Experimental setup view 4

5. Result and Discussion

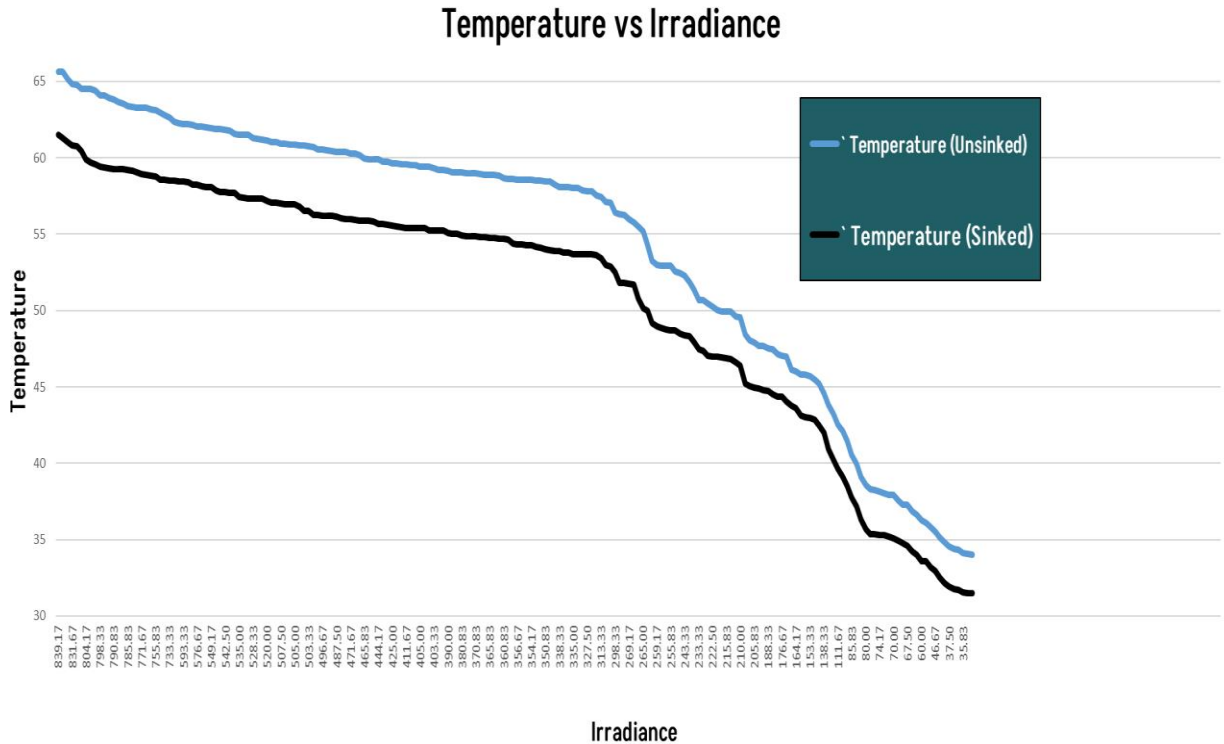### Section 5.1 Performance of Heat sink with Perforated fins

Figure 21 Temperature vs irradiance curve of perforated fin

During our experiment, data was collected for a period of fifteen days on solar panels equipped with and without perforated heat sinks. The purpose of this experiment was to compare the performance of sinked and unsinked solar panels.

After observing the temperature versus irradiance graph, a proportional relationship has been found out. As irradiance increased, the temperature of both unsinked and sinked panels also increased, and similar phenomenon occurred with the decreasing temperature.

When comparing the temperatures of unsunken and sunk panels, a discovery was made. The panel that was submerged consistently maintained a temperature 3 to 5 degrees Celsius lower than the panel that was not submerged. This indicates that the heat absorber successfully lowered the temperature of the solar panel.

The reduced temperature observed in the sunk panel can be attributed to the heat dissipation

properties of the finned heat sink. The heat sink's finned structure increases the available surface area for heat transfer. This increased surface area allows for more efficient heat dissipation, enabling the solar panel's generated heat to be transferred efficiently to the surrounding environment.

Our analysis concluded that the solar panel with the perforated fin heat sink was consistently cooler than the panel without a heat sink. This decrease in temperature is primarily attributable to the heat sink's enhanced heat dissipation capabilities, which effectively dissipate the heat generated by the solar panel and prevent an inordinate rise in temperature.
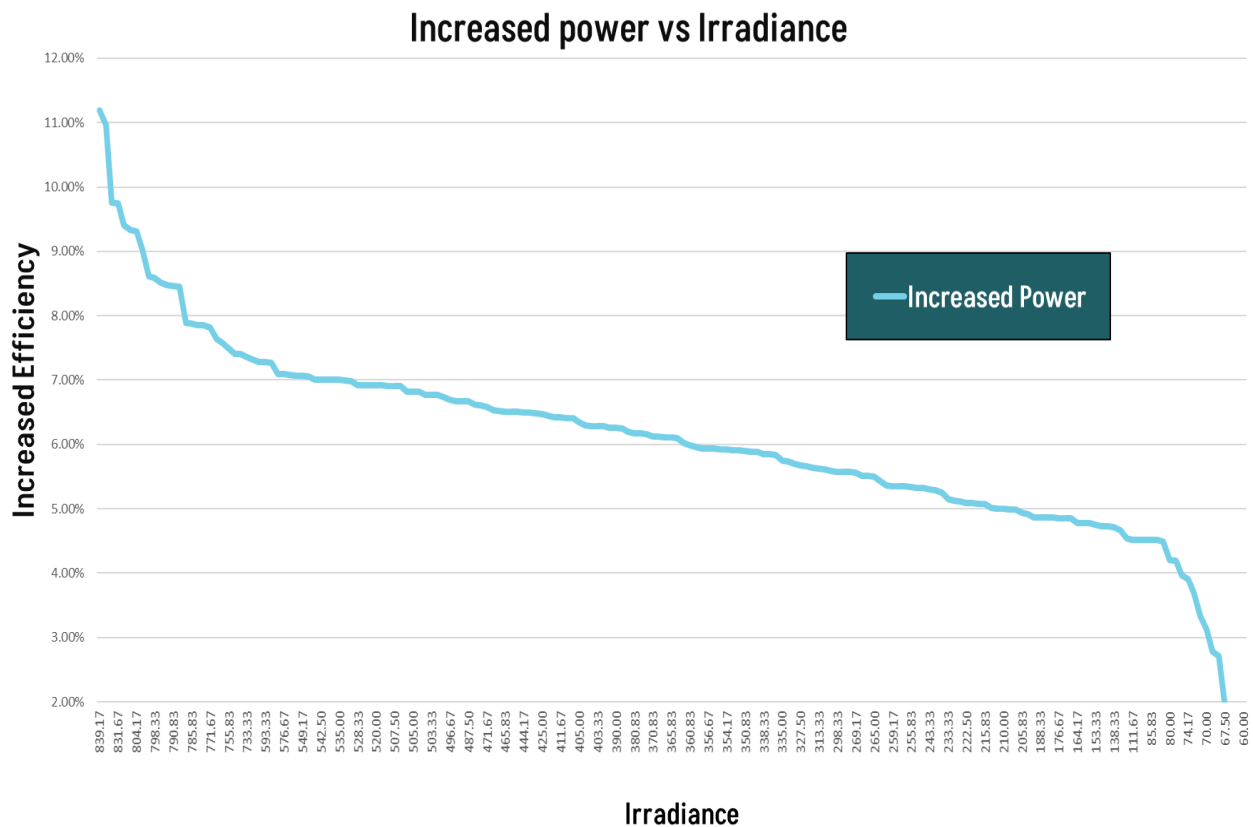
Figure 22 Increased efficiency vs irradiance curve of perforated fin

Our investigation examined the effect of perforated fins on the efficiency of solar panels in high-irradiance conditions. We discovered that when irradiance was high, the solar panel's efficiency increased by a remarkable 7–8%.

Several factors associated with the use of perforated fins contribute to this increase in effectiveness. First, the perforated fins contribute significantly to the solar panel's heat

dissipation. When the irradiance is high, the solar panel absorbs more sunlight and produces more electricity. This increased power output increases the panel's internal heat production. The presence of perforated fins improves thermal dissipation. Effectively increasing the surface area of the panel, the fins facilitate a more efficient heat transmission from the panel to the surrounding environment. Consequently, the temperature of the solar panel is maintained at a relatively low level, minimizing the negative effects of heat accumulation.

By sustaining a lower temperature, solar panels incur fewer thermal losses, thereby enhancing their overall performance. High temperatures can degrade the efficacy of solar panels, resulting in a decrease in their conversion efficiency. Utilizing perforated fins effectively modulates the solar panel's temperature, enabling it to operate within its optimal temperature range. Thus, electrical efficacy and overall efficiency are improved.

Additionally, the perforated fins reduce the likelihood of the solar panel developing hotspots. Hotspots can occur when certain regions of a solar panel experience higher temperatures than others, potentially resulting in a decrease in performance or panel failure. The enhanced heat dissipation provided by the perforated fins reduces the risk of flames by distributing heat more uniformly across the surface of the panel.

Under conditions of high irradiance, the use of perforated fins in solar panels results in a significant increase in efficiency. This is due to their ability to enhance heat dissipation, modulate panel temperature, minimize thermal losses, and reduce hotspots. By effectively regulating heat, the perforated fins maximize the solar panel system's electrical output and overall performance.
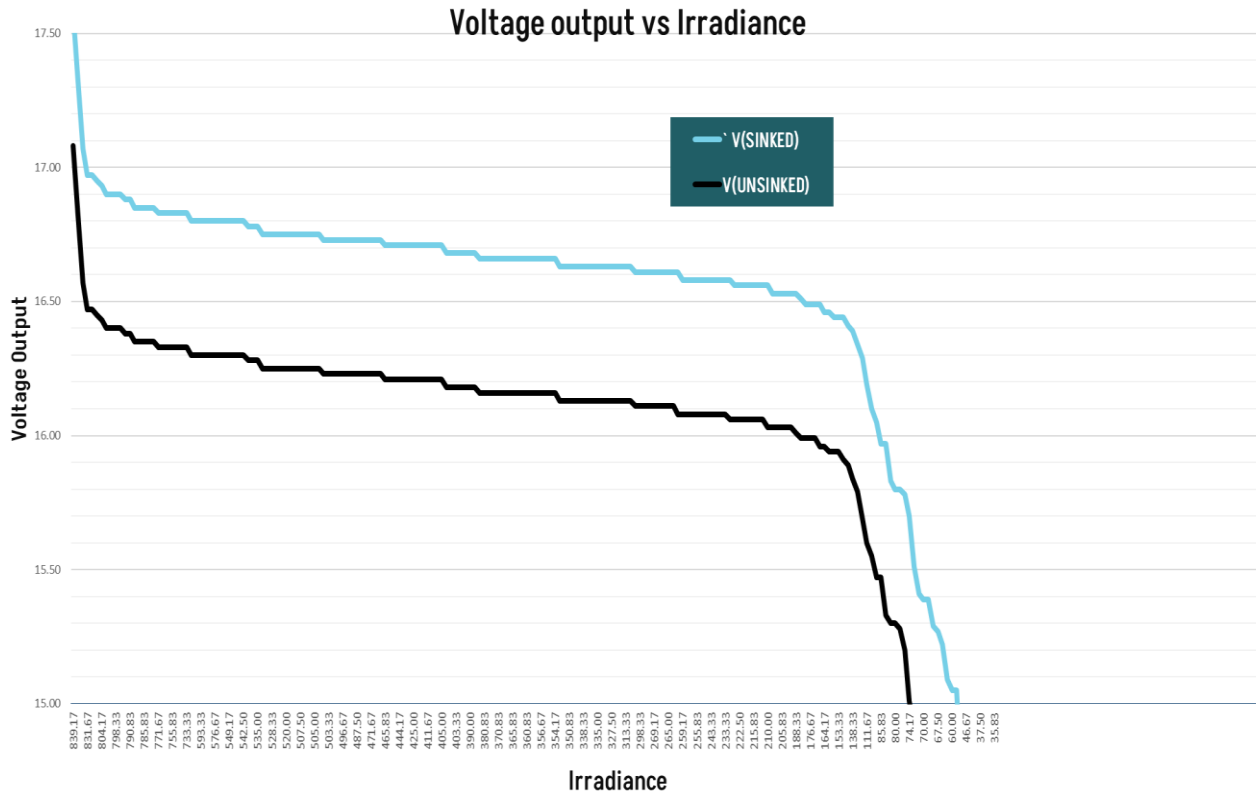
.

Figure 23 Voltage output vs irradiance curve of perforated fin

The voltage output of the sinked panel is consistently greater than that of the unsinked panel, as indicated by the graph analysis. In addition, under conditions of high irradiance, this difference in voltage output is amplified.

There are multiple factors that contribute to this phenomenon. First and foremost, the submerged panel benefits from the improved temperature regulation provided by the heat sink. As previously stated, the heat sink effectively dissipates the excess heat generated by the solar panel, preventing a temperature rise. Excessive heat can impair the electrical properties of the panel, including its voltage output.

Solar panels generate more electricity when exposed to high levels of irradiance. This increased power output is directly proportional to the output voltage of the panel. However, as power output increases, so does the temperature of the panel. Without the heat sink, the temperature of the unsinked panel rises more rapidly, resulting in greater thermal losses.

The submerging panel, on the other hand, maintains a lower temperature as a result of the heat sink's ability to facilitate heat dissipation. This reduces thermal losses and prevents overheating, allowing the panel to operate more efficiently. The panel with a condenser experiences less

voltage loss than the panel without one, resulting in a higher voltage output.

The graph demonstrates conclusively that the voltage output of the panel with a sink is consistently higher than that of the panel without a sink. This is due to the efficient temperature regulation of the heat sink, which minimizes thermal losses and prevents overheating. Under conditions of high irradiance, the ability of the chilled panel to maintain a lower temperature and operate more efficiently enables it to generate a higher voltage output.

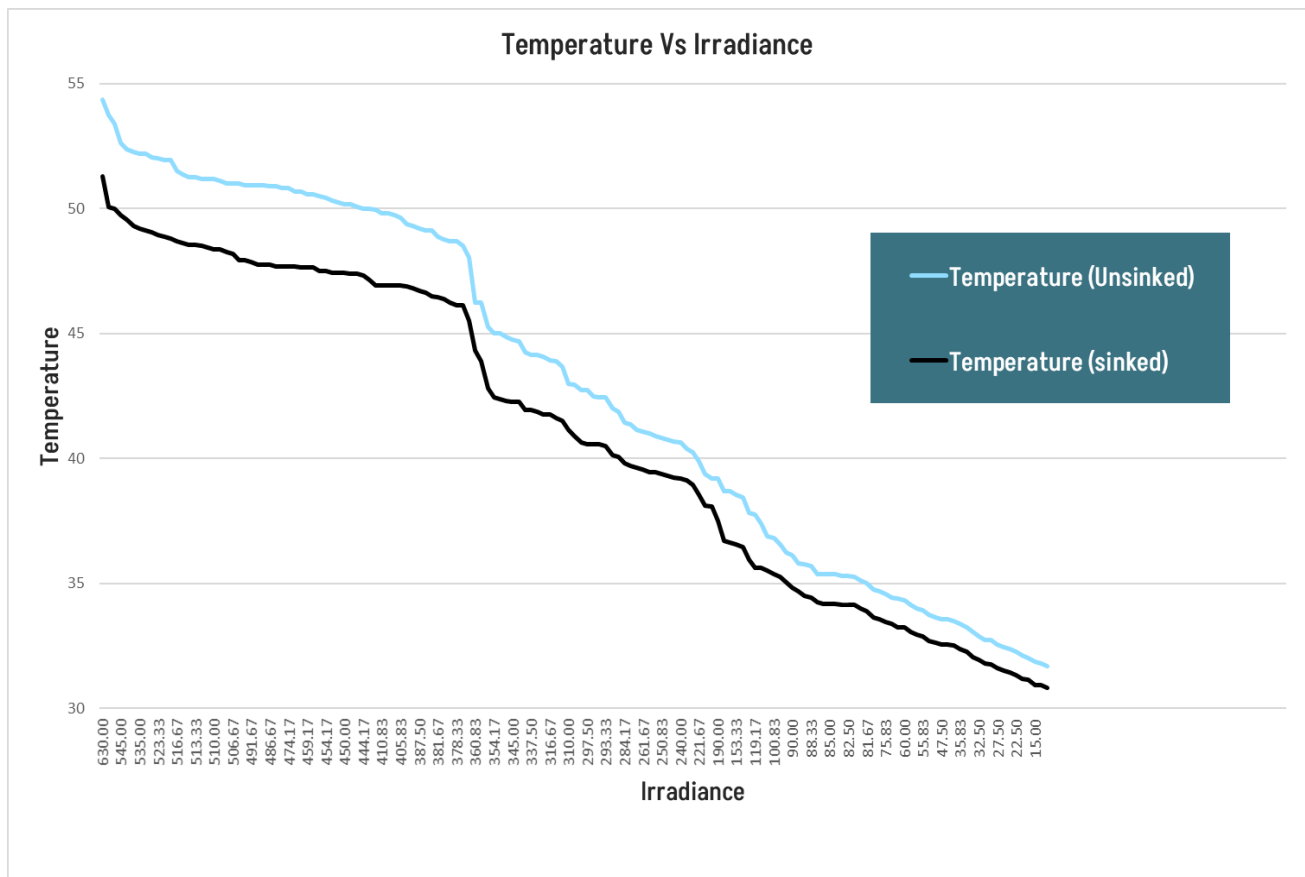**Section 5.2 Performance of Heat sink with plain fins**

Figure 24 Temperature vs irradiance curve of plain fin

In our investigation, we collected data on a solar panel heat sink with flat fins for fifteen days. Our objective was to ascertain the relationship between irradiance and temperature for panels with and without sinks.

Upon scrutinizing the graph of temperature versus irradiance, a distinct pattern was observed. It was evident that as the irradiance increased, the temperature of both unsinked and sink panels increased. As the irradiance began to decrease, the temperature of the panels increased. Throughout the duration of data collection, the unsinked panel consistently displayed greater

temperatures than the sinked panel. The temperature difference between the two panels ranged from 3 to 5 degrees Celsius. This indicates that the heat absorber successfully lowered the temperature of the solar panel.

By dissipating excess heat, the heat sink helps maintain a lower temperature within the sink panel. This is crucial because high temperatures can reduce the efficiency and durability of solar panels. Extreme heat can cause thermal stresses, the deterioration of electrical components, and a decrease in overall performance. With the heat sink present, however, the panel's temperature is maintained at a lower level, mitigating these negative effects.
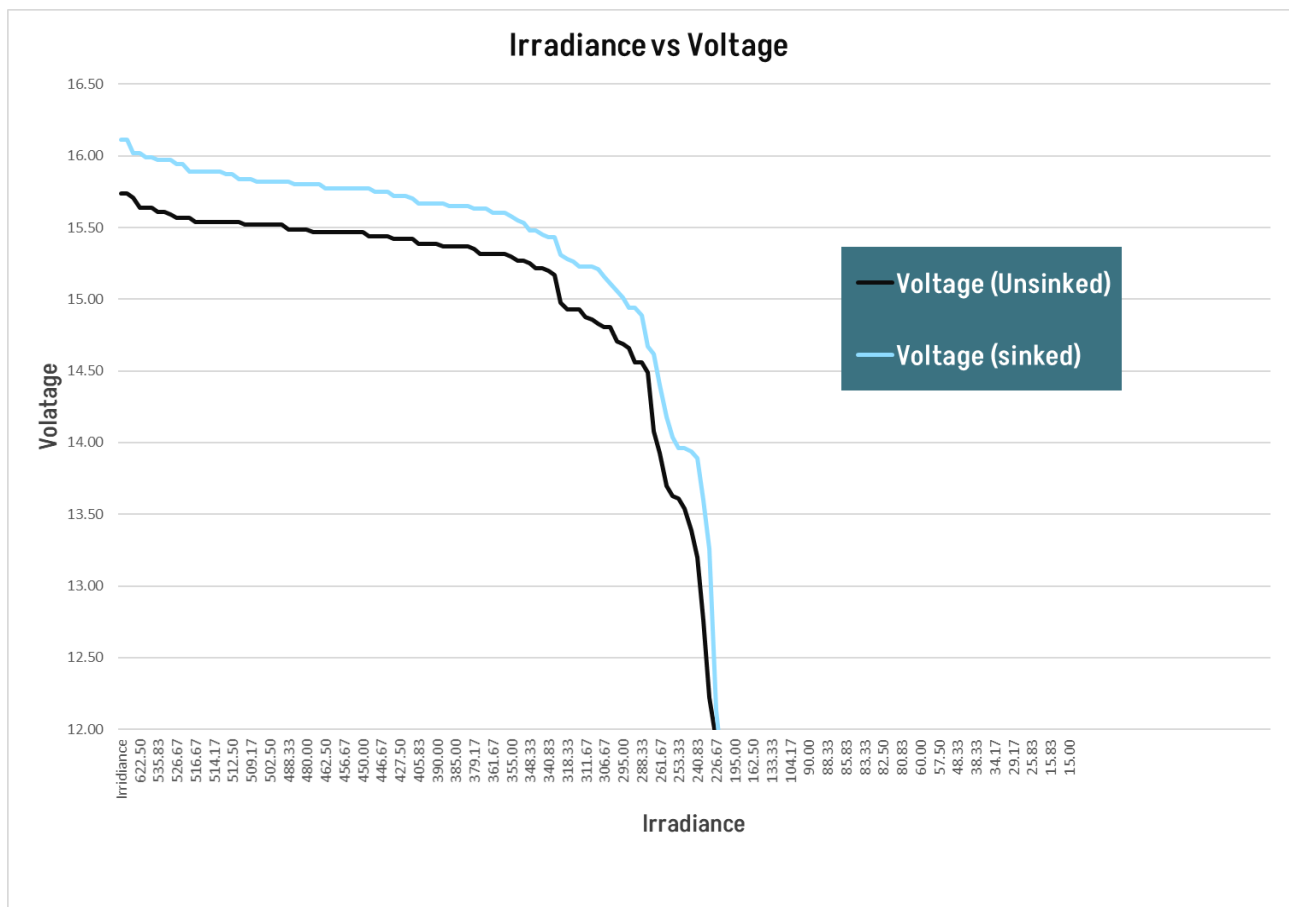
Figure 25 Irradiance vs voltage curve of plain fins

The analysis of the graph reveals that the voltage output of the flat plate-sinked panel consistently exceeds that of the unsinked panel, which is a significant finding. In addition, under conditions of high irradiance, this voltage difference becomes more pronounced.

Several factors contribute to this phenomenon's occurrence. First and foremost, the submerged panel benefits from the improved temperature regulation of the flat plate heat sink. As indicated

previously, the heat sink facilitates the efficient heat dissipation of the solar panel. By dissipating excess heat, the heat sink contributes to maintaining a lower temperature within the panel, which has a positive influence on its electrical properties, such as output voltage.

Under conditions of intense sunlight, the solar panel generates more electricity. The power production is directly proportional to the voltage output of the solar panel. However, as power output increases, so does the temperature of the panel. Without a heat sink, the temperature of the panel tends to rise rapidly, resulting in increased thermal losses.

Section 5.3 Comparative study between perforated and flat plate heatsinks
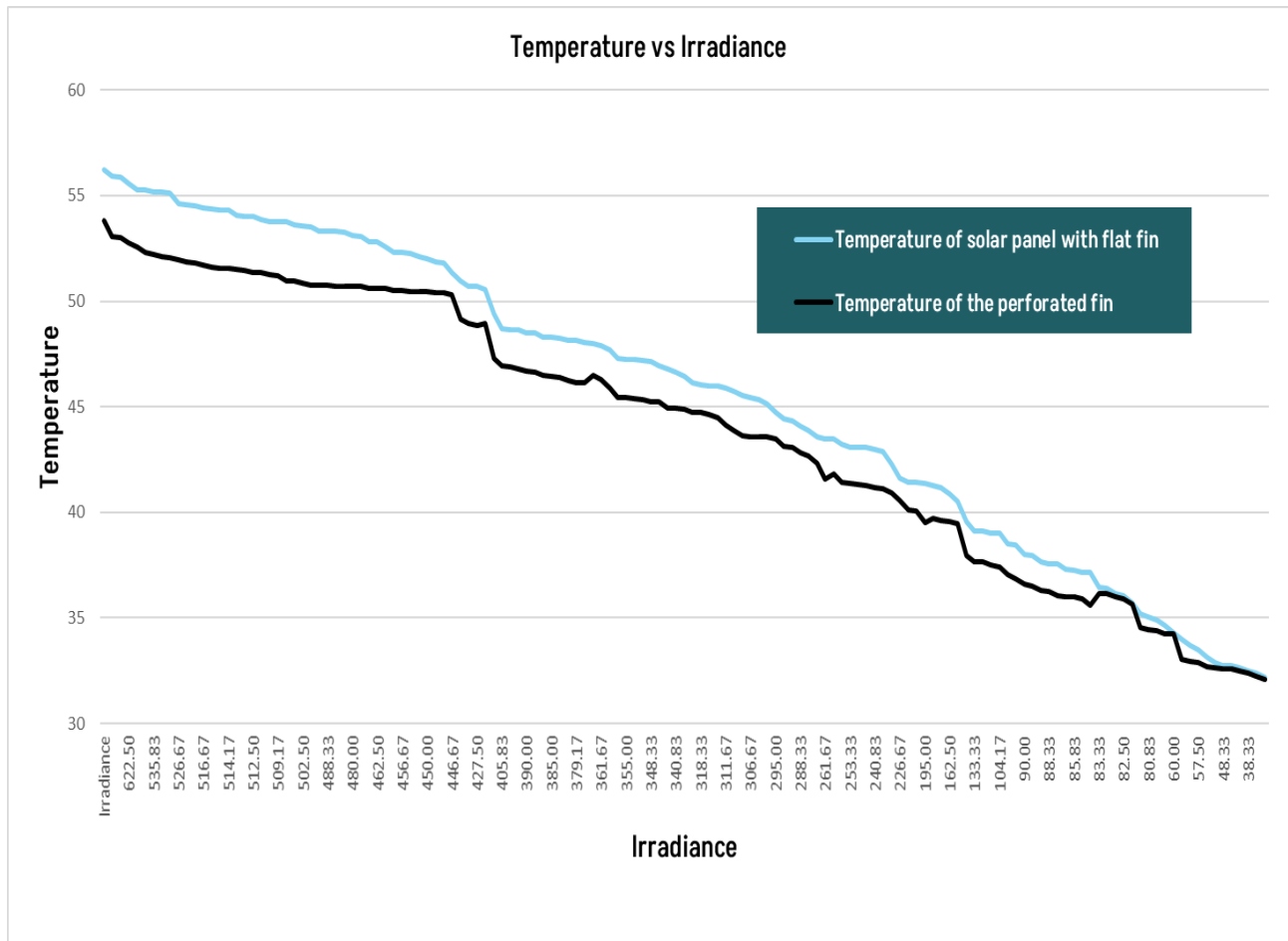
Figure 26 Temperature vs irradiance curve of perforated and plain fin

In a comparison of perforated and flat plate fin heat sinks, the superiority of the perforated fin heat sink became evident. This enhanced performance is primarily attributable to the improved natural convection airflow made possible by the design of perforated fins.

The effectiveness of a heat sink is extremely dependent on its ability to efficiently dissipate solar

panel heat. The mechanism for heat dissipation in the case of the flat plate fin heat sink is natural convection, where air circulation occurs naturally due to the temperature difference between the heat sink and its surroundings.

The design of the perforated fin heat sink enhances the natural convection circulation. The presence of perforations or openings in the structure of the fins allows for more efficient air circulation. This improves heat transfer and heat dissipation from the surface of the heat sink. The increased natural convection provided by the design of perforated fins has numerous advantages. It increases the available surface area for heat transfer, allowing for the dissipation of a higher amount of heat. This reduces the risk of overheating and its detrimental effects on the performance of the solar panel by lowering the temperatures within the heat sink and solar panel. Second, increased ventilation decreases thermal gradients within the heat sink. Thermal gradients can lead to irregular heat distribution, creating hotspots and decreasing the overall efficiency of the heat sink. The perforated fin heat sink reduces thermal gradients by promoting more uniform circulation, resulting in more efficient heat dissipation across the entire surface.

In addition, the increased ventilation helps to maintain a lower temperature within the heat sink by more efficiently removing heat. This prevents the heat sink from becoming overwhelmed, allowing it to continue dissipating heat efficiently and maintaining optimal operating conditions for the solar panel.

The comparative analysis concludes that the perforated fin heat sink outperforms the flat plate fin heat sink. The presence of perforations in the design of the fins enhances natural convection circulation, leading to increased heat transfer, decreased temperatures, and enhanced heat dissipation. Increased heat transfer surface area, reduced thermal gradients, and enhanced overall cooling performance are some of the advantages of the perforated fin design. These factors contribute to the superior performance of the perforated fin heat sink in removing heat from solar panels and maintaining their optimal operating conditions.

Section 5.4 Variation of temperature and voltage through out the day with the perforated heat sink

Sub Section 5.4.1 Based on data of 25th April

From 7:00 AM to 6:00 PM, the table displays the time of day, temperature, wind speed, and weather for each half-hour interval. "Haze," a term for a daylong meteorological phenomenon that denotes a marginally clouded atmosphere, is in effect. The data indicate that the temperature remained comparatively constant throughout the day, ranging from 27.78 to 33.89 degrees Celsius. The small temperature swings suggest that the solar panel is operating in a thermally stable environment.

It can be seen that irradiance, which stands for the amount of solar radiation incident on the panel's surface, follows a pattern that is consistent with daylight. The irradiance levels was maximum during the time period 10:30 to 1:30. The highest solar energy incident on the panel's surface occurs during this time, potentially resulting in greater energy generation.

As the daylight hours dwindled after 3 PM, the irradiance levels started to gradually decline. Overall, the research indicates that on April 25, between roughly 10:30 AM and 2 PM, the solar panel was exposed to high levels of irradiance and temperature. The temperature difference between the two panels within this timeframe was almost 4 to 5 degrees. This shows that throughout that time period, the conditions were ideal for the production of solar energy. The largest irradiance and temperature and also temperature change occur during midday hours when the sun is at its highest point in the sky, which is consistent with expectations.

However, the output voltage variation remained constant for the majority of the period. The difference in change in voltage output was close to 0.8-0.9V, which is consistent with the expected trend where the highest voltage production occurs during the noon hours when the irradiance levels are at their peak and within the optimal time period.

| Time	Temperature	Wind Speed	Condition
7:00 AM	27.22	3 mph	Haze
7:30 AM	27.22	9 mph	Haze
8:00 AM	27.78	8 mph	Haze
8:30 AM	27.78	7 mph	Haze
9:00 AM	27.78	6 mph	Haze
9:30 AM	28.89	5 mph	Haze
10:30 AM	31.11	7 mph	Haze
11:00 AM	32.22	5 mph	Haze
11:30 AM	32.78	9 mph	Haze
12:00 PM	32.78	7 mph	Haze
12:30 PM	33.89	12 mph	Haze
1:00 PM	33.89	14 mph	Haze
1:30 PM	35	12 mph	Haze
2:30 PM	36.11	9 mph	Haze
3:00 PM	36.11	8 mph	Haze
3:30 PM	36.11	12 mph	Haze
4:00 PM	36.11	12 mph	Haze
4:30 PM	35	12 mph	Haze
5:00 PM	33.89	9 mph	Haze
5:30 PM	33.89	9 mph	Haze
6:00 PM	33.89	8 mph	Haze
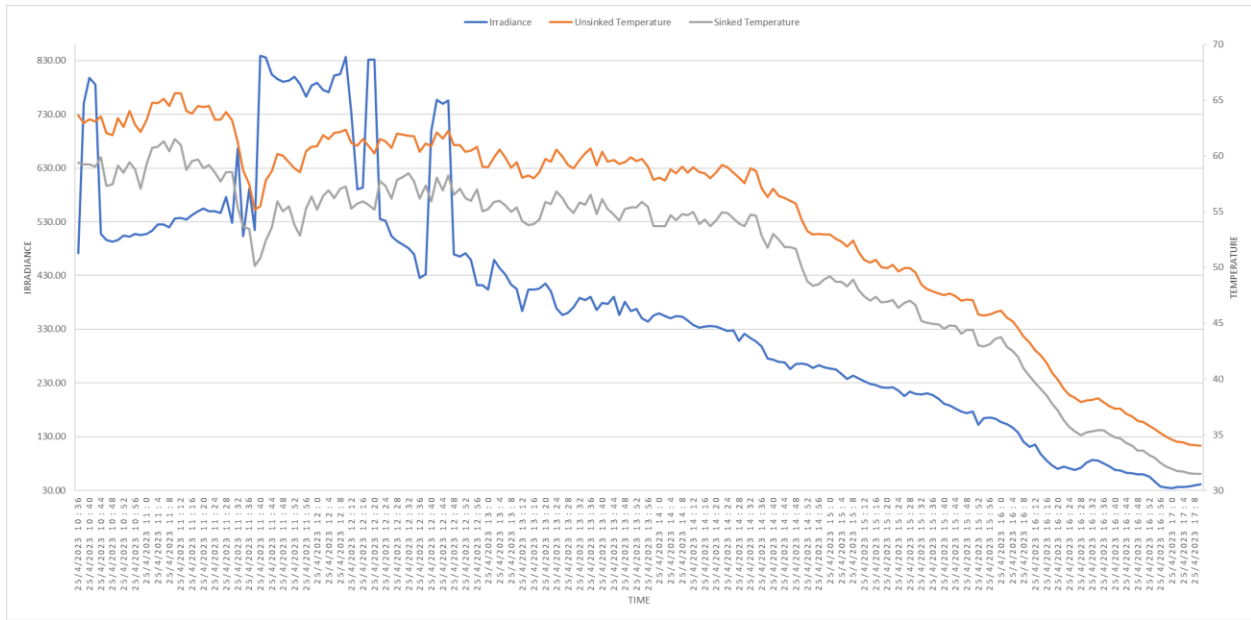
Figure 27:Irradiance vs temperature comparison graph of 25ᵗʰ april
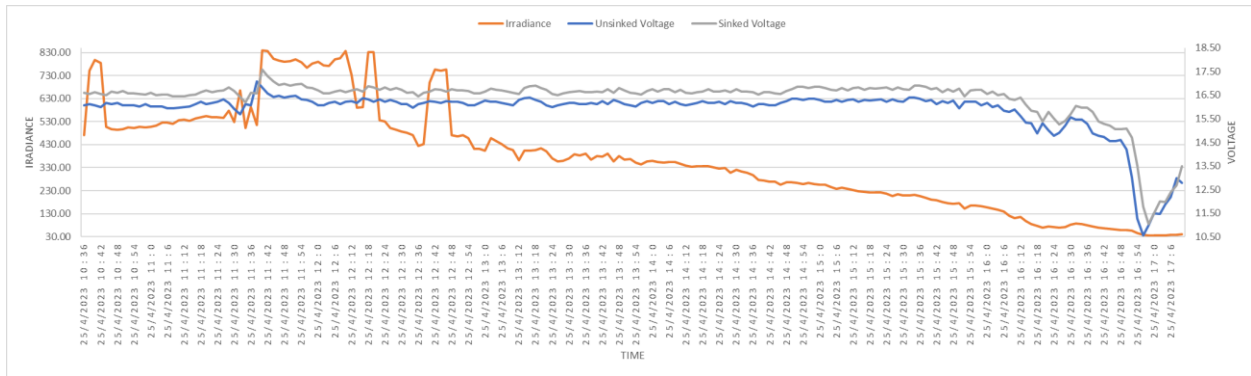

Figure 28:Irradiance vs Voltage comparison graph of 25ᵗʰ April

Sub Section 5.4.2 Based on data of 20th April

On April 20, the weather was the same all day long, with a haze signaling a marginally clouded atmosphere.

Let's talk about how two panels' temperatures and irradiance vary over time. Low sunlight energy at the start of the day led to relatively low irradiance levels. The two panels' temperatures, which were likewise noticeably lower, reflected this. The irradiance levels gradually increased as the daylight hours became longer, raising the temperatures of both panels as a result. The temperatures of the two panels rose to their maximum levels around midday when the irradiance was at its highest. The temperature variation between the two panels was around 4 to 4.5 degrees under ideal circumstances. The irradiance levels and temperatures of the two panels gradually decreased after peak hours as daylight hours began to shorten. The fact that there was a reasonably steady temperature difference across the panels, however, indicated that the thermal conditions were changing similarly for both of them.

The voltage outputs from both panels showed a degree of constancy throughout the day. For the bulk of the time intervals that were observed, they showed just minor fluctuations and remained largely steady. Even when the irradiance levels varied just slightly during the day, the panels' voltage outputs only slightly increased. This shows that the fluctuations in solar energy impacting on the panels' surfaces did not have a significant impact on the voltage output. Additionally, it was noted that for the bulk of the recorded time intervals, the voltage difference between the two panels' output voltages remained consistently less than 0.7 to 0.9 volt.

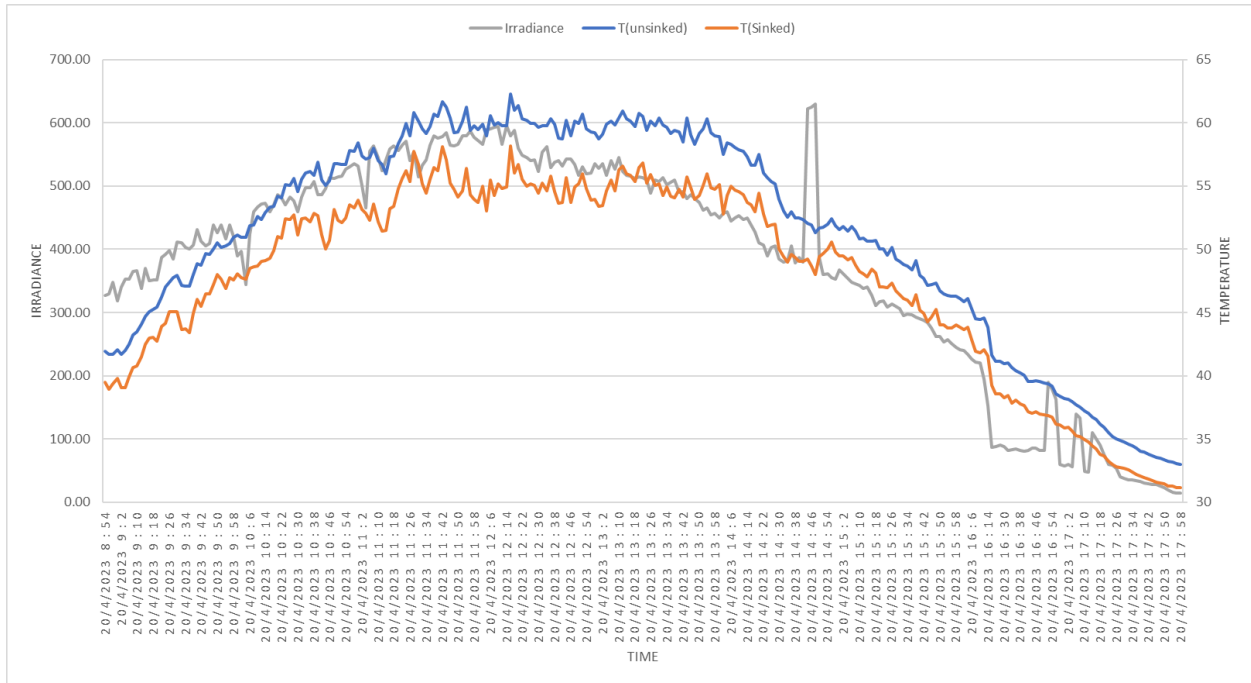| Time	Temperature	Wind Speed	Condition
7:00 AM	27.78	7 mph	Haze
7:30 AM	27.78	7 mph	Haze
8:00 AM	28.89	7 mph	Haze
8:30 AM	28.89	9 mph	Haze
9:00 AM	30	9 mph	Haze
9:30 AM	31.11	8 mph	Haze
10:00 AM	31.11	7 mph	Haze
10:30 AM	32.22	5 mph	Haze
11:00 AM	31.11	7 mph	Haze
11:30 AM	31.11	5 mph	Haze
12:00 PM	31.11	12 mph	Haze
12:30 PM	31.11	9 mph	Haze
1:00 PM	31.11	7 mph	Haze
1:30 PM	31.11	14 mph	Haze
2:00 PM	31.11	12 mph	Haze
2:30 PM	31.11	16 mph	Haze
3:00 PM	31.11	16 mph	Haze
3:30 PM	31.11	15 mph	Haze
4:00 PM	30	14 mph	Haze
4:30 PM	30	16 mph	Haze
5:00 PM	30	12 mph	Haze
5:30 PM	30	12 mph	Haze
6:00 PM	28.89	12 mph	Haze

Figure 29: Irradiance vs temperature comparison graph of 20th April
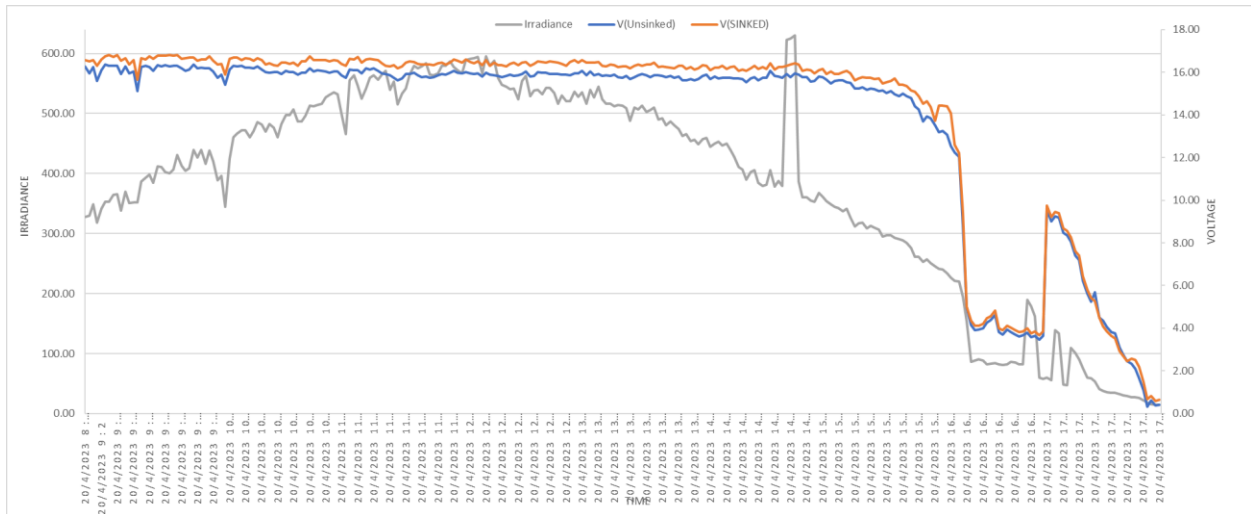

Figure 30: Irradiance vs voltage comparison graph of 20th April

Section 5.5 Variation of temperature and voltage through out the day with the flat fin heat sink

Sub Section 5.5.1 Based on data of 14th May

From 7:00 AM to 6:00 PM, the table displays the time of day, temperature, wind speed, and weather for each half-hour interval. "Haze," a term for a daylong meteorological phenomenon that denotes a marginally clouded atmosphere, is in effect. The data indicate that the temperature remained comparatively constant throughout the day, ranging from 27.78 to 32.22 degrees Celsius. The small temperature swings suggest that the solar panel is operating in a thermally stable environment.

It can be seen that irradiance, which stands for the amount of solar radiation incident on the panel's surface, follows a pattern that is consistent with daylight. The irradiance levels gradually increased between 7:00 AM and 11:30 AM, corresponding to the lengthening of daylight. The irradiation values were relatively low but steadily increased during this time. The peak daylight hours were from 11:50 AM to 2:45 PM, when the irradiance levels were constantly high. The highest solar energy incident on the panel's surface occurs during this time, potentially resulting in greater energy generation. As the daylight hours dwindled after 3 PM, the irradiance levels started to gradually decline. Overall, the research indicates that on April 14, between roughly 11:30 AM and 2:45 PM, the solar panel was exposed to high levels of irradiance and temperature. The temperature difference between the two panels within this timeframe was almost 2 degrees. This shows that throughout that time period, the conditions were ideal for the production of solar energy. The largest irradiance and temperature and also temperature change occur during midday hours when the sun is at its highest point in the sky, which is consistent with expectations.

However, the output voltage variation remained constant for the majority of the period. The difference in change in voltage output was close to 0.5 to 0.6 volt, which is consistent with the expected trend where the highest voltage production occurs during the noon hours when the irradiance levels are at their peak and within the optimal time period.

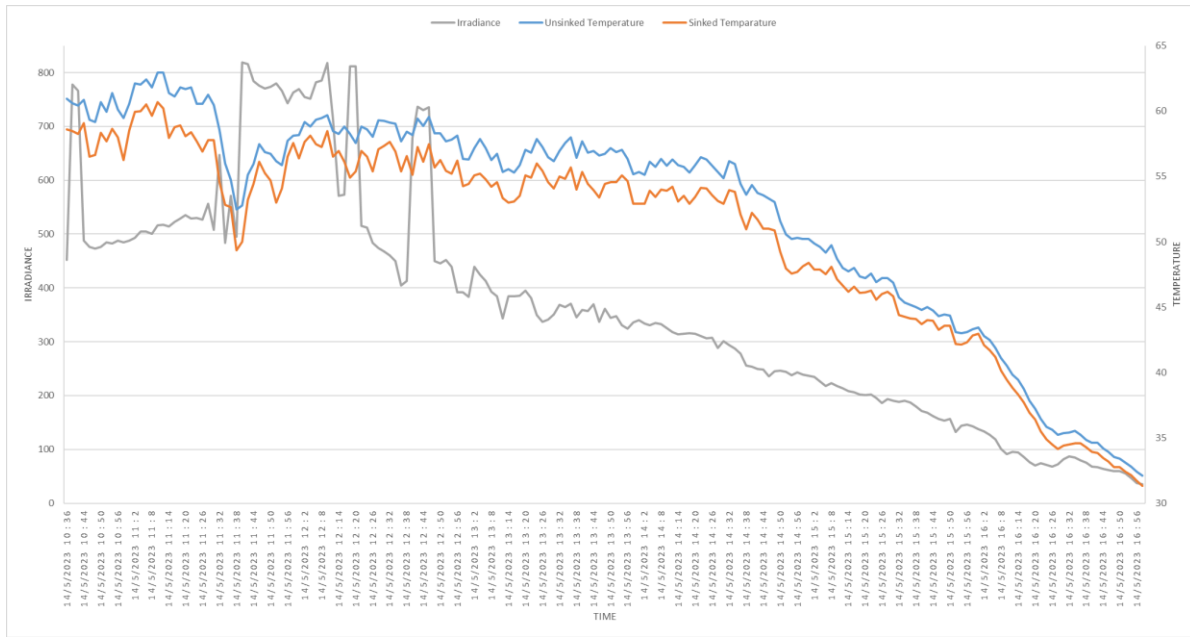| Time	Temperature	Wind Speed	Condition
7:00 AM	27.78	7 mph	Haze
7:30 AM	27.78	7 mph	Haze
8:00 AM	28.89	7 mph	Haze
8:30 AM	28.89	9 mph	Haze
9:00 AM	30	9 mph	Haze
9:30 AM	31.11	8 mph	Haze
10:00 AM	31.11	7 mph	Haze
10:30 AM	32.22	5 mph	Haze
11:00 AM	31.11	7 mph	Haze
11:30 AM	31.11	5 mph	Haze
12:00 PM	31.11	12 mph	Haze
12:30 PM	31.11	9 mph	Haze
1:00 PM	31.11	7 mph	Haze
1:30 PM	31.11	14 mph	Haze
2:00 PM	31.11	12 mph	Haze
2:30 PM	31.11	16 mph	Haze
3:00 PM	31.11	16 mph	Haze
3:30 PM	31.11	15 mph	Haze
4:00 PM	30	14 mph	Haze
4:30 PM	30	16 mph	Haze
5:00 PM	30	12 mph	Haze
5:30 PM	30	12 mph	Haze
6:00 PM	28.89	12 mph	Haze

Figure 31: Irradiance vs temperature comparison graph of 14th May
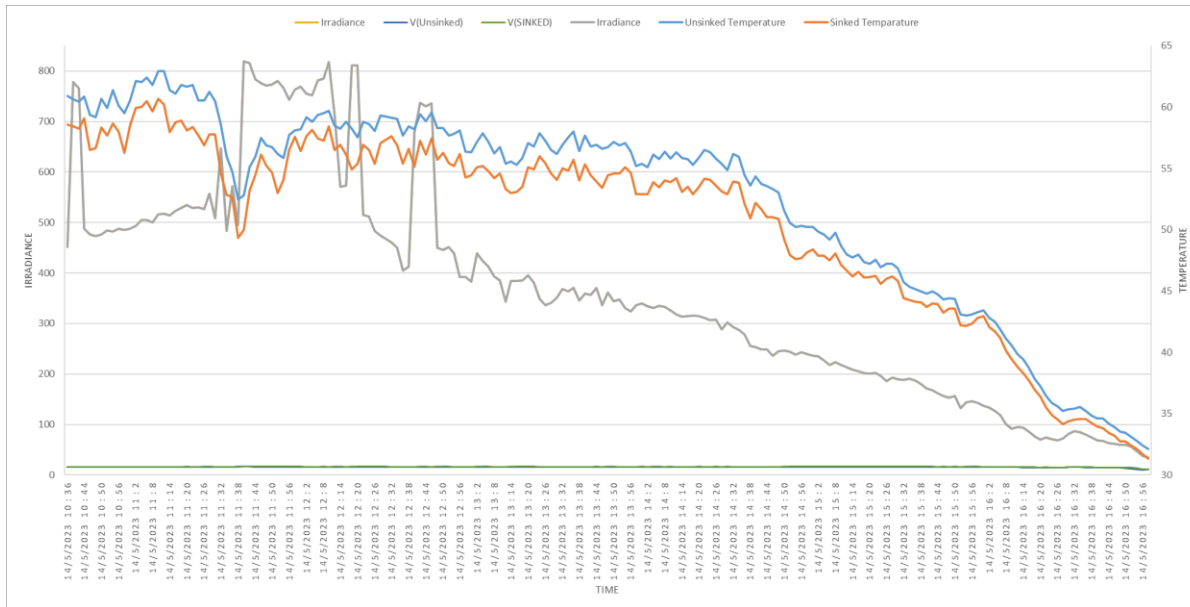

Figure 32: Irradiance vs voltage comparison graph of 14th May

Sub Section 5.5.2 Based on data of 17th May

On April 17, the weather was the same all day long, with a haze signaling a marginally occluded atmosphere.

Let's talk about how two panels' temperatures and irradiance vary over time. Low sunlight energy at the start of the day led to relatively low irradiance levels. The two panels' temperatures, which were likewise noticeably lower, reflected this. The irradiance levels gradually increased as the daylight hours became longer, raising the temperatures of both panels as a result. The temperatures of the two panels rose to their maximum levels around midday when the irradiance was at its highest. The temperature variation between the two panels was over 2 degrees under ideal circumstances. An explanation for this temperature differential can be found in the panel orientation, shade, and efficiency. The irradiance levels and temperatures of the two panels gradually decreased after peak hours as daylight hours began to shorten. The fact that there was a reasonably steady temperature difference across the panels, however, indicated that the thermal conditions were changing similarly for both of them.

The voltage outputs from both panels showed a degree of constancy throughout the day. For the bulk of the time intervals that were observed, they showed just minor fluctuations and remained largely steady. Even when the irradiance levels varied just slightly during the day, the panels' voltage outputs only slightly increased. This shows that the fluctuations in solar energy impacting on the panels' surfaces did not have a significant impact on the voltage output. Additionally, it was noted that for the bulk of the recorded time intervals, the voltage difference between the two panels' output voltages remained consistently less than 1 volt. Both panels' voltage outputs were fairly stable throughout the day. They showed just slight variations and were essentially constant throughout the vast majority of the time periods studied .The panels' voltage outputs barely marginally increased even when the irradiance levels fluctuated somewhat during the day. This demonstrates that the voltage output was not significantly affected by the variations in solar energy striking the panels' surfaces. The difference in output voltage between the two panels was around 0.5 volt for the vast majority of the measured timespan. Even during the optimal period, when irradiance levels and temperatures were at their peak, the voltage difference between the panels was close to 1 volt. This indicates that there was little difference in the voltage outputs of the two panels, suggesting that their electrical performance and qualities were equivalent

| Time	Temperature	Wind Speed	Condition
7:00 AM	25	3 mph	Haze
7:30 AM	26.11	3 mph	Haze
8:00 AM	27.22	6 mph	Haze
8:30 AM	27.78	5 mph	Haze
9:00 AM	28.89	5 mph	Haze
9:30 AM	26.11	25 mph	T-Storm / Windy
10:00 AM	25	14 mph	T-Storm
10:30 AM	25	14 mph	T-Storm
11:00 AM	27.22	17 mph	T-Storm
11:30 AM	27.22	12 mph	Haze
12:00 PM	27.78	9 mph	Haze
12:30 PM	27.78	12 mph	Haze
1:00 PM	27.78	14 mph	Haze
1:30 PM	28.89	14 mph	Haze
2:00 PM	30	9 mph	Haze
2:30 PM	31.11	8 mph	Haze
3:00 PM	31.11	7 mph	Haze
3:30 PM	32.22	12 mph	Haze
4:00 PM	32.22	14 mph	Haze
4:30 PM	32.22	7 mph	Haze
5:00 PM	32.22	9 mph	Haze
5:30 PM	32.22	9 mph	Haze
6:00 PM	31.11	9 mph	Haze
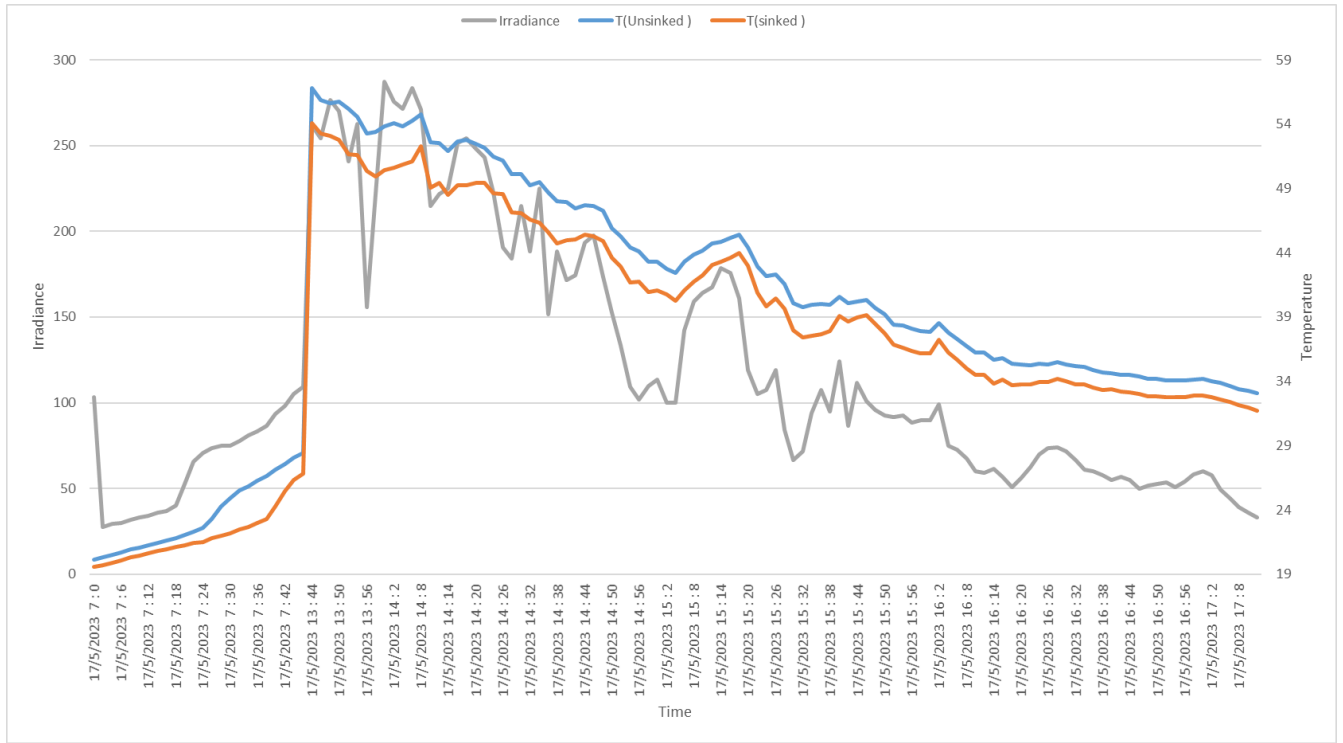
Figure 33: Irradiance vs temperature comparison graph of 17th May
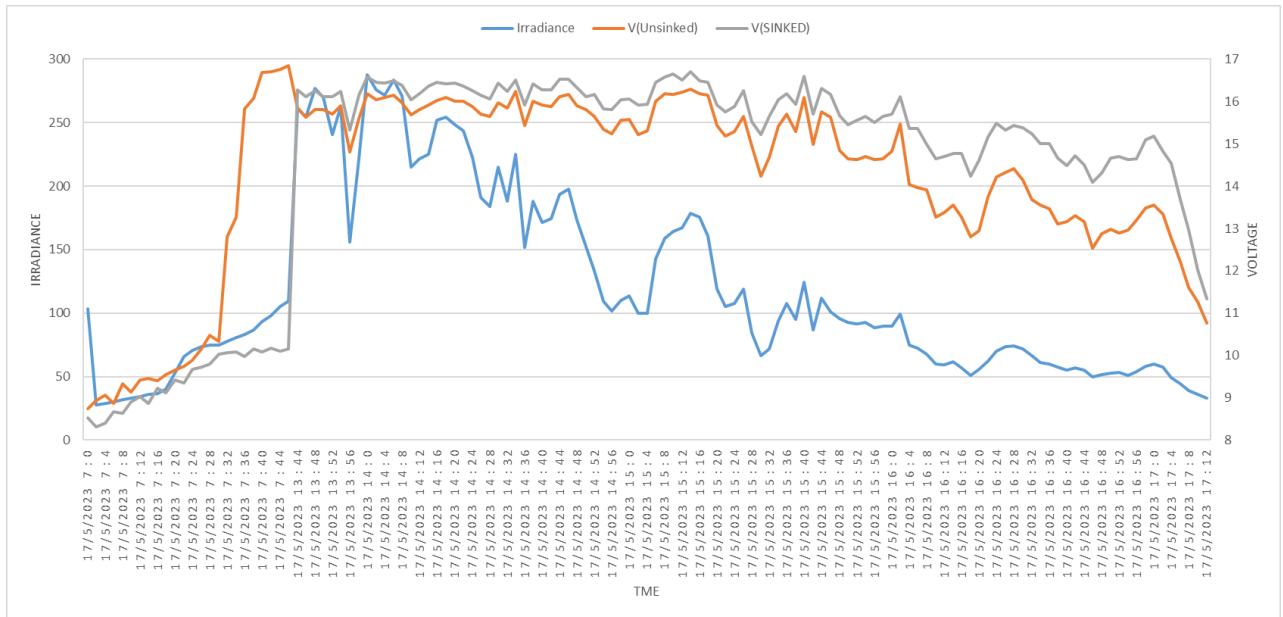

Figure 34: Irradiance vs voltage comparison graph of 17th May

6. Conclusion

Solar panels with a heat sink are demonstrably more efficient than panels without a heat sink, according to a comprehensive study. In addition, the efficacy of the perforated fin is superior to that of the flat plate fin among the two fin types examined.

The primary objective of this study was to evaluate the impact of adding a heat absorber to solar panels on their efficacy. The results consistently demonstrated that solar panels with a heat absorber were more efficient than those without. This is due to the ability of the heat sink to effectively dissipate the excess heat produced by the solar panel, thereby preventing temperature rise and mitigating thermal losses.

Additionally, the study aimed to evaluate the effectiveness of two distinct fin designs, perforated fin and flat plate fin. The analysis revealed that the solar panel with the perforated fin was more effective than the one with the flat plate fin.

Several factors contribute to the superior effectiveness of the perforated fin. Initially, the presence of perforations within the structure of the fin improves natural convection circulation. By enhancing heat transfer, this improved ventilation promotes more efficient cooling of the solar panel.

In addition to increasing heat dissipation surface area, the perforated fin design decreases thermal gradients. The larger surface area allows for a more efficient heat transmission, resulting in a cooler operating temperature for the panel. This optimizes the panel's electrical performance and prevents any adverse effects caused by excessive heat.

Additionally, the perforated fin design diminishes thermal gradients, resulting in a more uniform distribution of heat across the surface of the heat sink. This reduces the likelihood of hotspots and increases heat dissipation efficiency.

Overall, the study demonstrates that adding a heat absorber to solar panels substantially enhances their efficiency. In addition, the perforated fin design enhances the solar panel's overall performance more effectively than the flat plate fin design. Improved circulation, increased surface area, and reduced thermal gradients all contribute to the perforated fin's superior performance.

This study demonstrates conclusively that the use of a heat absorber increases the efficiency of solar panels. In terms of efficacy, the findings indicate that the perforated fin design is superior to the flat plate fin design. These findings contribute to ongoing efforts to maximize the

efficiency of solar panels and highlight the importance of selecting the most appropriate heat sink designs for solar panel applications.

7. Reference

[1] U. Nations, "ClimateChange," *United Nations*. https://www.un.org/en/climatechange (accessed Jan. 15, 2023).

[2] "Global warming | Definition, Causes, Effects, Solutions, & Facts | Britannica." https://www.britannica.com/science/global-warming (accessed Jan. 15, 2023).

[3] "Fossil fuels and climate change: the facts." https://www.clientearth.org/latest/latest-updates/stories/fossil-fuels-and-climate-change-the-facts/ (accessed Jan. 15, 2023).

[4] "Solar energy - Electricity generation | Britannica." https://www.britannica.com/science/solar-energy/Electricity-generation (accessed Jan. 15, 2023).

[5] J. Yang, J. Li, Z. Yang, and Y. Duan, "Thermodynamic analysis and optimization of a solar organic Rankine cycle operating with stable output," *Energy Conversion and Management*, vol. 187, pp. 459–471, May 2019, doi: 10.1016/j.enconman.2019.03.021.

[6] "Photovoltaic Energy Factsheet," *Center for Sustainable Systems*. https://css.umich.edu/publications/factsheets/energy/photovoltaic-energy-factsheet (accessed Jan. 15, 2023).

[7] S. Wu and C. Xiong, "Passive cooling technology for photovoltaic panels for domestic houses," *International Journal of Low-Carbon Technologies*, vol. 9, no. 2, pp. 118–126, Jun. 2014, doi: 10.1093/ijlct/ctu013.

[8] M. Usama Siddiqui, A. F. M. Arif, L. Kelley, and S. Dubowsky, "Three-dimensional thermal modeling of a photovoltaic module under varying conditions," *Solar Energy*, vol. 86, no. 9, pp. 2620–2631, Sep. 2012, doi: 10.1016/j.solener.2012.05.034.

[9] E. Skoplaki, A. G. Boudouvis, and J. A. Palyvos, "A simple correlation for the operating temperature of photovoltaic modules of arbitrary mounting," *Solar Energy Materials and Solar Cells*, vol. 92, no. 11, pp. 1393–1402, Nov. 2008, doi: 10.1016/j.solmat.2008.05.016.

[10] M. Kumar and A. Kumar, "Performance assessment and degradation analysis of solar photovoltaic technologies: A review," *Renewable and Sustainable Energy Reviews*, vol. 78, pp. 554–587, Oct. 2017, doi: 10.1016/j.rser.2017.04.083.

[11] J. Zhou, Z. Zhang, H. Liu, and Q. Yi, "Temperature distribution and back sheet role of polycrystalline silicon photovoltaic modules," *Applied Thermal Engineering*, vol. 111, pp. 1296–1303, Jan. 2017, doi: 10.1016/j.applthermaleng.2016.10.095.

[12] Y. Cui *et al.*, "Organic photovoltaic cell with 17% efficiency and superior processability," *National Science Review*, vol. 7, no. 7, pp. 1239–1246, Jul. 2020, doi: 10.1093/nsr/nwz200.

[13] X. Han, Y. Wang, and L. Zhu, "The performance and long-term stability of silicon concentrator solar cells immersed in dielectric liquids," *Energy Conversion and Management*, vol. 66, pp. 189–198, Feb. 2013, doi: 10.1016/j.enconman.2012.10.009.

[14] L. pauly, L. Rekha, C. V. Vazhappilly, and C. R. Melvinraj, "Numerical Simulation for Solar Hybrid Photovoltaic Thermal Air Collector," *Procedia Technology*, vol. 24, pp. 513–522, Jan. 2016, doi: 10.1016/j.protcy.2016.05.088.

[15] A. Abhat, "Low temperature latent heat thermal energy storage: Heat storage materials," *Solar Energy*, vol. 30, no. 4, pp. 313–332, Jan. 1983, doi: 10.1016/0038-092X(83)90186-X.

[16] H. M. S. Bahaidarah, A. A. B. Baloch, and P. Gandhidasan, "Modeling and comparative analysis of jet impingement cooling and conventional channel cooling for photovoltaic strings," in *2014 IEEE 40th Photovoltaic Specialist Conference (PVSC)*, Jun. 2014, pp. 0748–0753. doi: 10.1109/PVSC.2014.6925028.

[17] W. G. Anderson, P. M. Dussinger, D. B. Sarraf, and S. Tamanna, "Heat pipe cooling of concentrating photovoltaic cells," in *2008 33rd IEEE Photovoltaic Specialists Conference*, May 2008, pp. 1–6. doi: 10.1109/PVSC.2008.4922577.

[18] S. Mehrotra, P. Rawat, M. Debbarma, and K. Sudhakar, "Performance of a solar panel with water immersion cooling technique".

[19] S. G. Kandlikar, "High Flux Heat Removal with Microchannels—A Roadmap of Challenges and Opportunities," *Heat Transfer Engineering*, vol. 26, no. 8, pp. 5–14, Oct. 2005, doi: 10.1080/01457630591003655.

[20] G. Hetsroni, A. Mosyak, Z. Segal, and G. Ziskind, "A uniform temperature heat sink for cooling of electronic devices," *International Journal of Heat and Mass Transfer*, vol. 45, no. 16, pp. 3275–3286, Jul. 2002, doi: 10.1016/S0017-9310(02)00048-0.

[21] C. Min, C. Nuofu, Y. Xiaoli, W. Yu, B. Yiming, and Z. Xingwang, "Thermal analysis and test for single concentrator solar cells," *J. Semicond.*, vol. 30, no. 4, p. 044011, Apr. 2009, doi: 10.1088/1674-4926/30/4/044011.

[22] J. A. Gotmare, D. S. Borkar, and P. R. Hatwar, "Experimental Investigation of PV panel with fin cooling under natural convection," no. 02, 2015.

[23] E. Cuce, T. Bali, and S. A. Sekucoglu, "Effects of passive cooling on performance of silicon

photovoltaic cells," *International Journal of Low-Carbon Technologies*, vol. 6, no. 4, pp. 299–308, Dec. 2011, doi: 10.1093/ijlct/ctr018.

[24] School of Environment and Energy Engineering, Beijing University of Civil Engineering and Architecture, Beijing 100044 China, H. Chen, X. Chen, S. Li, and H. Ding, "Comparative study on the performance improvement of photovoltaic panel with passive cooling under natural ventilation," *ijsgce*, 2014, doi: 10.12720/sgce.3.4.374-379.

[25] A. M. A. Soliman, H. Hassan, M. Ahmed, and S. Ookawara, "A 3d model of the effect of using heat spreader on the performance of photovoltaic panel (PV)," *Mathematics and Computers in Simulation*, vol. 167, pp. 78–91, Jan. 2020, doi: 10.1016/j.matcom.2018.05.011.

[26] J. Kim and Y. Nam, "Study on the Cooling Effect of Attached Fins on PV Using CFD Simulation," *Energies*, vol. 12, no. 4, Art. no. 4, Jan. 2019, doi: 10.3390/en12040758.

[27] F. Bayrak, H. F. Oztop, and F. Selimefendigil, "Effects of different fin parameters on temperature and efficiency for cooling of photovoltaic panels under natural convection," *Solar Energy*, vol. 188, pp. 484–494, Aug. 2019, doi: 10.1016/j.solener.2019.06.036.

[28] I. Hasan, "Enhancement the Performance of PV Panel by Using Fins as Heat Sink," *ETJ*, vol. 36, no. 7A, pp. 798–805, Jul. 2018, doi: 10.30684/etj.36.7A.13.

[29] G. Marco Tina, "Simulation Model of Photovoltaic and Photovoltaic/Thermal Module/String Under Nonuniform Distribution of Irradiance and Temperature," *Journal of Solar Energy Engineering*, vol. 139, no. 2, Dec. 2016, doi: 10.1115/1.4035152.

[30] Arifin, Z. *et al.* (2020) 'Numerical and experimental investigation of air cooling for photovoltaic panels using aluminum heat sinks', *International Journal of Photoenergy*, 2020, pp. 1–9. doi:10.1155/2020/1574274.

[31] Elbreki, A.M. *et al.* (2021) 'Experimental and economic analysis of passive cooling PV module using fins and planar reflector', *Case Studies in Thermal Engineering*, 23, p. 100801. doi:10.1016/j.csite.2020.100801.